



Research paper

Sulfonyl-containing phenyl-pyrrolyl pentane analogues: Novel non-secosteroidal vitamin D receptor modulators with favorable physicochemical properties, pharmacokinetic properties and anti-tumor activity



Zi-Sheng Kang¹, Cong Wang¹, Xiao-Lin Han, Bin Wang, Hao-Liang Yuan, Si-Yuan Hou, Mei-Xi Hao, Jun-Jie Du, Yan-Yi Li, An-Wei Zhou, Can Zhang*

State Key Laboratory of Natural Medicines, Jiangsu Key Laboratory of Drug Discovery for Metabolic Diseases, Center of New Drug Discovery, China Pharmaceutical University, 24 Tong Jia Xiang, Nanjing, 210009, China

ARTICLE INFO

Article history:

Received 14 July 2018

Received in revised form

27 August 2018

Accepted 28 August 2018

Available online 31 August 2018

Keywords:

Vitamin D receptor (VDR)

Non-secosteroidal

Physicochemical properties

Pharmacokinetic properties

Anti-tumor activity

ABSTRACT

Modulating the vitamin D receptor (VDR) is an effective way to treat for cancer. We previously reported a potent non-secosteroidal VDR modulator (**sw-22**) with modest anti-tumor activity, which could be due to its undesirable physicochemical and pharmacokinetic properties. In this study, we investigated the structure-activity and structure-property relationships around the 2'-hydroxyl group of **sw-22** to improve the physicochemical properties, pharmacokinetic properties and anti-tumor activity. Compounds **19a** and **27b**, the potent non-secosteroidal VDR modulators, were identified as the most effective molecules in inhibiting the proliferation of three cancer cell lines, particularly breast cancer cells, with a low IC_{50} via the distribution of cell cycle and induction of apoptosis by stimulating the expression of p21, p27 and Bax. Further investigation revealed that **19a** and **27b** possessed favorable rat microsomal metabolic stability (2.22 and 2.3 times, respectively, more stable than **sw-22**), solubility (43.9 and 50.2 times, respectively, more soluble than **sw-22**) and *in vivo* pharmacokinetic properties. In addition, **19a** and **27b** showed excellent *in vivo* anti-tumor activity without cause hypercalcemia, which is the main side effect of marketed VDR modulators. In summary, the favorable physicochemical properties, pharmacokinetic properties and anti-tumor activity of **19a** and **27b** highlight their potential therapeutic applications in cancer treatment.

© 2018 Elsevier Masson SAS. All rights reserved.

1. Introduction

Vitamin D receptor (VDR), a member of the steroid–thyroid–retinoid receptor superfamily of ligand-activated transcription factors, which involve regulating calcium homeostasis and bone metabolism [1–3]. Recently, accumulating evidence suggests that VDR was involved in antineoplastic actions in various malignancies, such as breast, pancreatic and prostate cancer [4–8]. After being combined with its modulator, VDR dimerizes with the retinoid X receptor (RXR) and binds to the vitamin D response elements (VDREs) to alter the rate of target gene transcription. With

recruitment of co-modulators, the activated VDR can decrease tumor growth mainly by suppressing proliferation or promoting apoptosis of cancer cells [9,10]. In order to enable VDR play a more effective antineoplastic activity, large numbers of VDR modulators had been applied to anti-tumor researches [11–14].

The VDR modulators can be classified into “secosteroid” and “non-secosteroidal” based on their structure specificity. Up to now, more than 3000 secosteroidal VDR modulators (SVDRMs) have been developed, such as calcipotriol (**1**), tacalcitol (**2**) and natural VDR modulator 1,25(OH)₂D₃ (**3**) [15]. However, secosteroidal-based chemical synthesis has proven to be difficult and costly [16]. What's more, in clinical cancer treatment, the required doses of these SVDRMs induced serious hypercalcemia, the main side effect of VDR modulators which could induce abdominal pain, kidney stones and cardiac arrest [17]. In addition, clinical studies showed that 20 to 30 percent of cancer patients suffer from hypercalcemia at the

* Corresponding author.

E-mail address: zhangcan@cpu.edu.cn (C. Zhang).

¹ The first two authors contributed equal.

same time, which strongly limit the clinical application of SVDRMs in cancer treatment [18–21].

In order to potentiate beneficial properties of SVDRMs and avoid their disadvantages, non-secosteroidal VDR modulators (NVDRMs) were developed, such as LG190178 (**4**) and CB-16 (**5**) [22]. NVDRMs are easy to synthesis, and possess distinct activities compared with SVDRMs, including VDR binding affinity and VDR-dependent transcriptional activation. More importantly, NVDRMs can carry out their physiological functions without hypercalcemia side effect even at high doses [23,24].

Recently, we successfully designed and characterized a novel series of NVDRM bearing phenyl-pyrrolyl pentane scaffold [25–27]. Among them, compound **sw-22** (**6**), the most potent NVDRM, showed EC_{50} value for inducing the HL-60 leukaemia cells differentiation in 1.06 nM, which is better than positive control tacalcitol (**2**). Furthermore, in *in vivo* study, **sw-22** showed no significant change on serum calcium [25]. However, **sw-22** showed modest anti-tumor activity in *in vitro* and *in vivo* studies, which may be due to its undesirable metabolic stability ($t_{1/2} = 25.76$ min, rat liver microsomes), solubility (1.7 $\mu\text{g}/\text{mL}$, pH 7.4) and *in vivo* pharmacokinetics property ($t_{1/2} = 2.89$ h, intravenous; $t_{1/2} = 3.47$ h, intraperitoneal). Compound **sw-22** contain a 2-hydroxy-3,3-dimethylbutoxy side chain at phenyl part, the 2'-hydroxyl group on this side chain could form hydrogen bonds with amino acid residues (His 393) of the VDR ligand binding domain (LBD), which is important to VDR transcriptional activity. However, the hydroxyl group on the side chain of VDR modulators is easy to be oxidated [28], which could lead to its inactive and therefore causing undesirable metabolic stability and pharmacokinetic properties of **sw-22**. Accordingly, we hypothesized that suitable chemical modification around the 2'-hydroxyl group could improve the physicochemical and pharmacokinetic properties of **sw-22**, and therefore, lead to the analogues possess better anti-tumor activity.

In this work, our first effort was aimed at identifying a suitable group to replace the 2'-OH group on the side chain based on **sw-22** (see Fig. 1). Sulfonyl group commonly used as a group to improve the metabolic stability and solubility of molecules [29] and furthermore, the oxygen atoms on the sulfonyl group could act as hydrogen bond acceptors, which could form hydrogen bonds with amino acid residues and mimic the function of 2'-OH group on the side chain. Consequently, we replaced the 2'-OH group to sulfonyl group while replacing the substituents in the terminal of side chain, and targeting improved physicochemical properties (i.e., metabolic stability and solubility) as well as anti-tumor activity. Then, hydrophilic groups were added to the pyrrol part, which could form hydrogen bonds with amino acid residues of VDR LBD. Next, to explore the effects of substitutions at terminal of side chain and oxidation state of sulfur group, compounds **19a-b** and **20a** were designed. Additionally, in order to investigate the influence of the substitution positions of the pyrrole ring, phenyl-pentane group on C-4 position of pyrrole ring instead of C-5 position was designed and obtained compounds **26a-b**, **27a-b** (Fig. 2). Furthermore, the *in vitro* and *in vivo* biological activities of these non-secosteroidal VDR modulators are evaluated in this study.

2. Results and discussion

2.1. Chemistry

The synthetic pathway of target compounds **15a-o**, **16a-l** and **17a-k** is outlined in Scheme 1. Key intermediate **7** was readily prepared using our previously reported approach. Compound **7** coupling with 1*H*-pyrrole-2-carboxylate in the presence of lewis acid $\text{BF}_3 \cdot \text{Et}_2\text{O}$ at 0 °C produced the intermediate **8**, following the treatment with iodoethane in DMF to afford intermediate **9**. Subsequently, reduction of compound **9** offered compound **10**, then

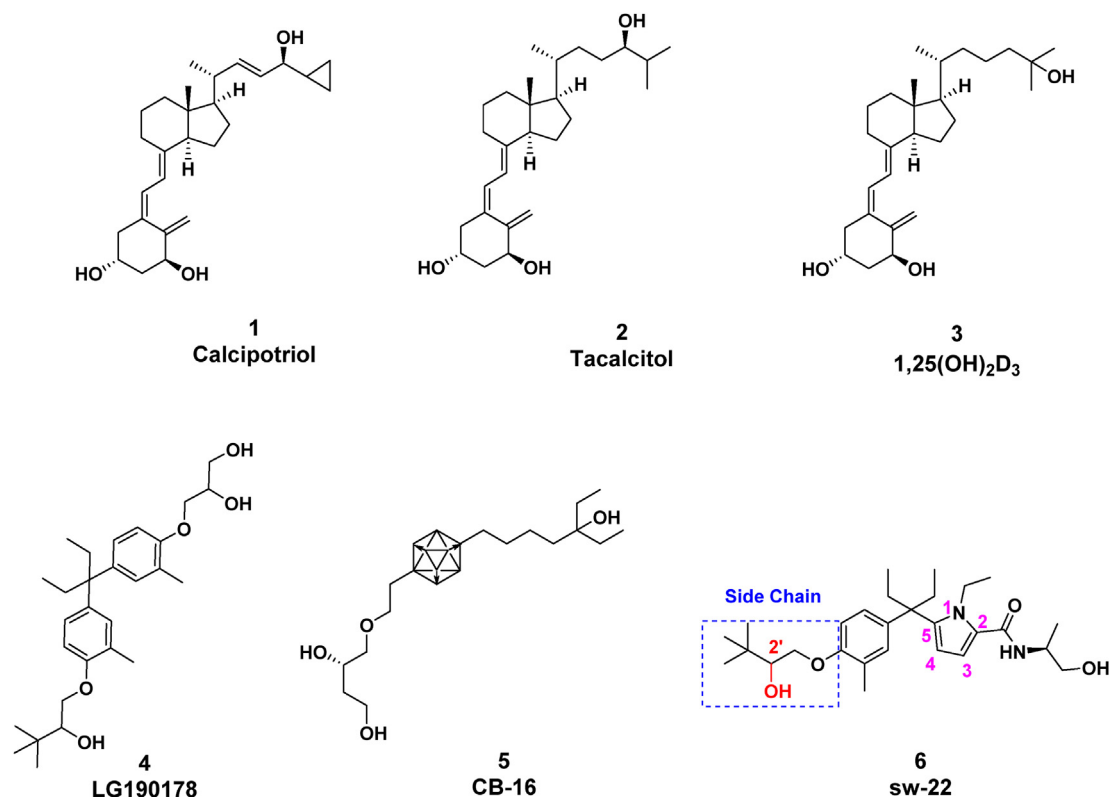


Fig. 1. Chemical structures of VDR modulators.

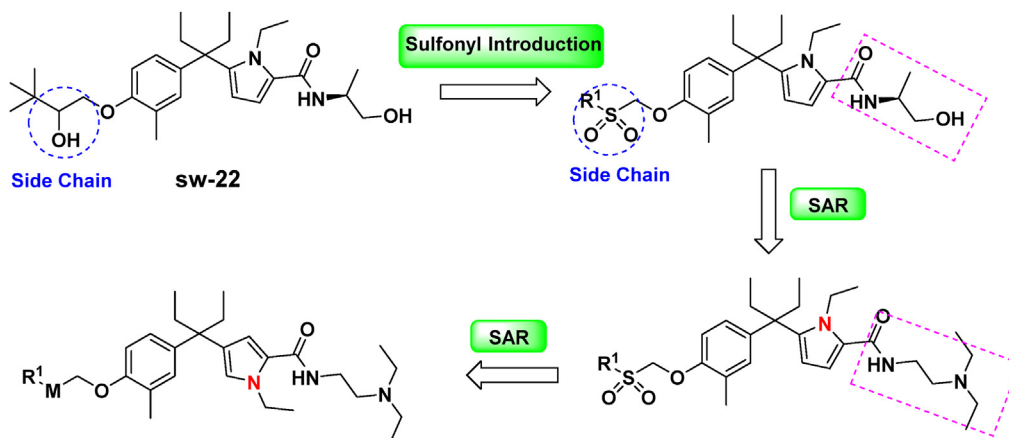


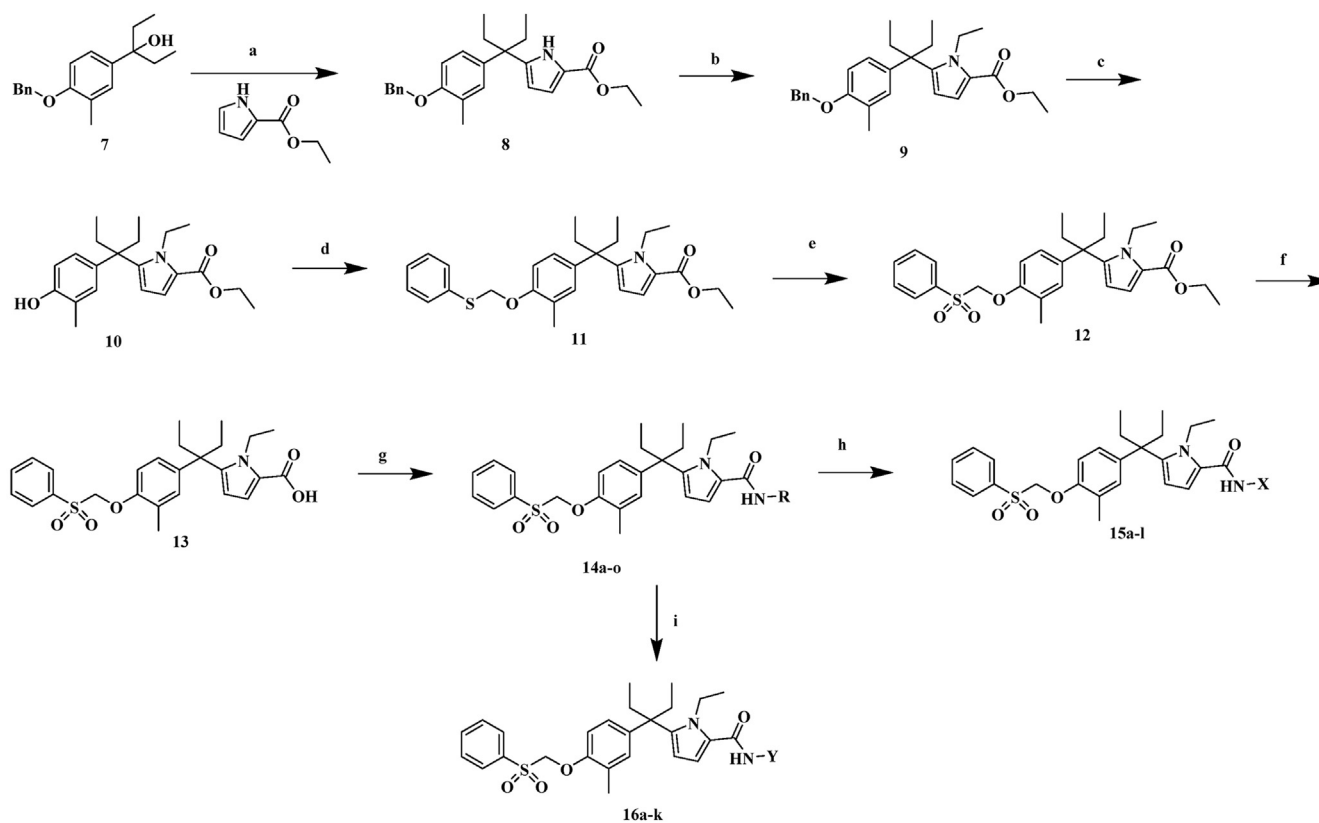
Fig. 2. Design concept of novel non-secosteroidal VDR modulators.

compound **10** was dissolved in DMF in the presence of chloromethyl phenyl sulfide to give compound **11**. The oxidation reaction of compound **11** obtained the intermediate **12**, which was hydrolyzed by NaOH to give **13**. By reaction of intermediate **13** with the corresponding amines, intermediates **14a-o** were produced. Finally, reduction or hydrolysis of appropriate esters group in **14a-l**, the target compounds **15a-l** and **16a-k** were obtained, respectively.

The synthetic pathway of target compounds **19a-b** and **20a** is outlined in Scheme 2. Hydrolysis of compound **10** by KOH produced the intermediate **17** in the presence of carboxyl group. Substitution of the carboxyl group with *N,N*-

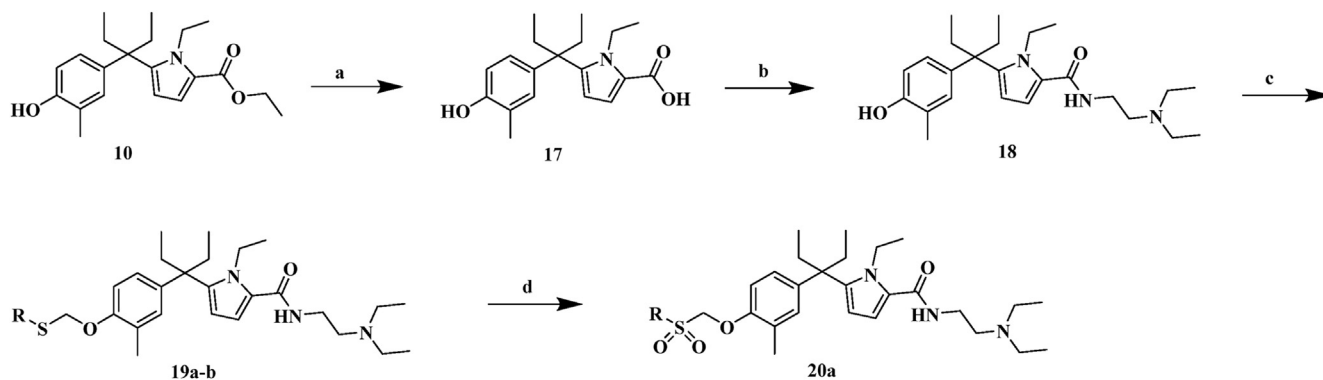
diethylethylenediamine provide the compound **18**. Compounds **19a-b** were prepared in a single step by the treatment of compound **18** with different halogen substituted alkyl sulfide. By oxidation of compound **19a**, the target compound **20a** was obtained.

The synthetic pathway of target compounds **26a-b** and **27a-b** is outlined in Scheme 3. Intermediate **21**, which was the regioselectivity isomer of intermediate **8**, was produced by reacting with ethyl pyrrole-2-carboxylate in the presence of lewis acid $\text{BF}_3 \cdot \text{Et}_2\text{O}$ at 20 °C. Compound **21** treated with iodoethane in DMF to afford intermediate **22**. The reduction reaction of compound **22** obtained the intermediate **23**, which were hydrolyzed by KOH to give **24**. By



Scheme 1. Synthesis of target compounds **14a-o**, **15a-l** and **16a-k**.

^aReagents and conditions: (a) ethyl *1H*-pyrrole-2-carboxylate, $\text{BF}_3 \cdot \text{Et}_2\text{O}$, -20–0 °C, 3 h; (b) $\text{C}_2\text{H}_5\text{I}$, NaH, DMF, 0–25 °C, 5 h; (c) Pd/C, H_2 , MeOH, 25 °C, 12 h; (d) chloromethyl phenyl sulfide, NaH, DMF, 0–70 °C, 12 h; (e) potassium peroxymonosulfate, EtOH/ H_2O (10:1), 25 °C, 24 h; (f) NaOH, EtOH/ H_2O (10:1), 90 °C, 24 h; (g) EDCI, HOBT, TEA, RNH_2 , DCM, rt, overnight; (i) NaBH_4 , MeOH, 0–25 °C, 8 h; (j) KOH, MeOH/ H_2O (10:1), 70 °C, 24 h.



Scheme 2. Synthesis of target compounds **19a-b** and **20a**^d.

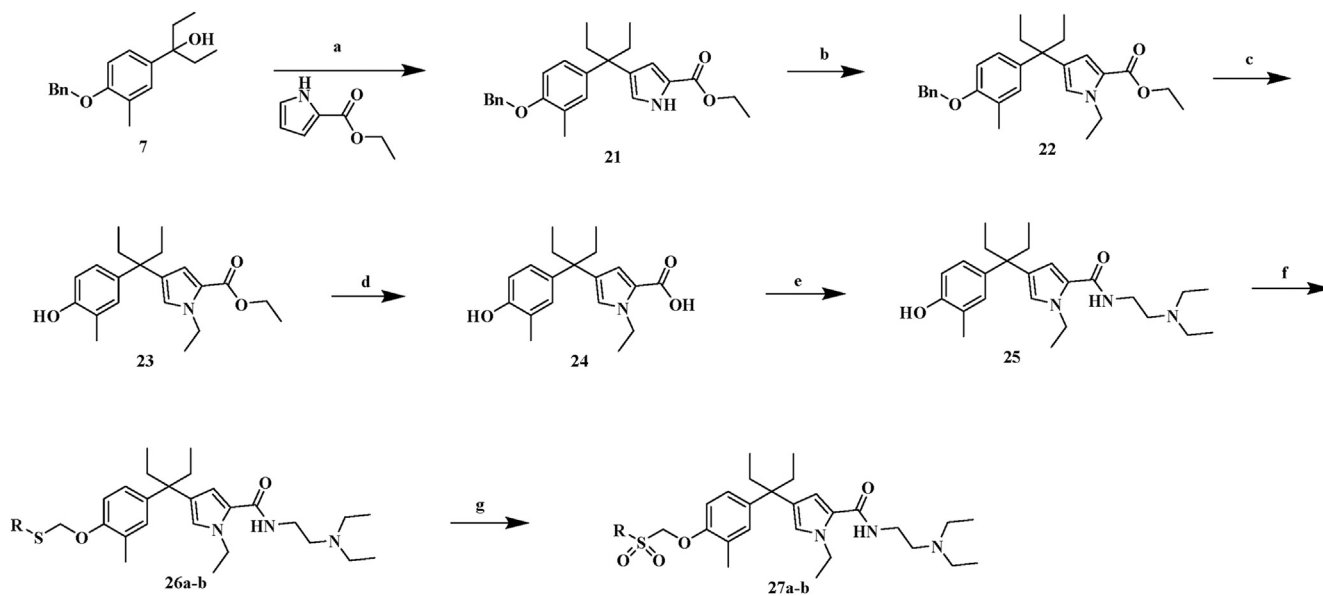
^aReagents and conditions: (a) NaOH, EtOH/H₂O (10:1), 90 °C, 24 h; (b) EDCI, HOBt, TEA, *N,N*-diethylethane-1,2-diamine, DCM, rt, overnight; (c) chloromethyl sulfide, NaH, DMF, 0–70 °C, 12 h; (d) potassium peroxymonosulfate, EtOH/H₂O (10:1), 25 °C, 24 h.

reaction of intermediate **24** with *N,N*-diethylethylenediamine, intermediates **25** was produced. Compounds **26a-b** were prepared in a single step by the treatment of compound **25** with different halogen substituted alkyl sulfide. By oxidation of compounds **26a-b**, the target compounds **27a-b** were obtained, respectively.

2.2. In vitro antiproliferative activity screening and SARs analysis

The structures of synthesized compounds are shown in Table 1. And the effect of these synthesized compounds on cell proliferation was investigated in a panel of human cancer cell lines from diverse tissue origins by MTT assay, the IC₅₀ values are listed in Table 2. Replacing the 2'-OH group with sulfonyl group (15a) led to a modest improvement in potency, maintained VDR binding affinity (Table 3) and more importantly, the better physicochemical properties (Table 4). Given these results, we decided to proceed with the sulfonyl group for the next round of analogues which were aimed at modifying the hydrophilic groups in the pyrrole part. Introduction of different amino acid esters decreased cytotoxicity. Next, we focused on exploring SAR at the α -position of amide bond by replacing the

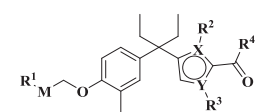
methyl group with various steric bulk groups as well as varying the chiral in this portion of the molecule. The steric bulk of the α -position modulated the potency, and the methyl group was the optimal group for the antiproliferative effect (**15a-g**). And introducing another chain contain hydroxyl group at this position is unfavorable (**15i-l**). In addition, oxidative product **16a-k** was devoid of activity, similar detrimental effect was observed in compounds with methyl ester group at terminal of this side chain, which suggest that carboxyl acid and methyl ester groups may not preferred. Our biggest potency improvement occurred when we introduced the *N,N*-diethylpropan-1-amine chain in the pyrrole part (**14o**), which had an IC₅₀ value of 6.27 μ M, 4.68 μ M and 7.13 μ M for BXP-3, MCF-7 and PC-3 cells, respectively. Given these results, we decided to proceed with the *N,N*-diethylpropan-1-amine chain for the next round of analogues. Changes in substituents at the terminal of side chain at phenyl part affected activity, replaced of the phenyl group with the methyl group result in decreased activity (**20a**), and change oxidation state of sulfur group can not improve activity. Exploration of the SAR around the substitution positions of the pyrrole ring indicated that substitution at the C-4 position was



Scheme 3. Synthesis of target compounds **26a-b** and **27a-b**^d.

^aReagents and conditions: (a) ethyl 1*H*-pyrrole-2-carboxylate, BF₃·Et₂O, 30 °C, 3 h; (b) C₂H₅I, NaH, DMF, 0–25 °C, 5 h; (c) Pd/C, H₂, MeOH, 25 °C, 12 h; (d) NaOH, EtOH/H₂O (10:1), 90 °C, 24 h; (e) EDCI, HOBt, TEA, *N,N*-diethylethane-1,2-diamine, DCM, rt, overnight; (f) chloromethyl sulfide, NaH, DMF, 0–70 °C, 12 h; (g) potassium peroxymonosulfate, EtOH/H₂O (10:1), 25 °C, 24 h.

Table 1
The structures of all target compounds.



Compd.	R ¹	M	X	Y	R ²	R ³	R ⁴
14a	C ₆ H ₅		N	C	C ₂ H ₅	H	
14b	C ₆ H ₅		N	C	C ₂ H ₅	H	
14c	C ₆ H ₅		N	C	C ₂ H ₅	H	
14h	C ₆ H ₅		N	C	C ₂ H ₅	H	
14i	C ₆ H ₅		N	C	C ₂ H ₅	H	
14m	C ₆ H ₅		N	C	C ₂ H ₅	H	
14n	C ₆ H ₅		N	C	C ₂ H ₅	H	
14o	C ₆ H ₅		N	C	C ₂ H ₅	H	
15a	C ₆ H ₅		N	C	C ₂ H ₅	H	
15b	C ₆ H ₅		N	C	C ₂ H ₅	H	
15c	C ₆ H ₅		N	C	C ₂ H ₅	H	
15d	C ₆ H ₅		N	C	C ₂ H ₅	H	
15e	C ₆ H ₅		N	C	C ₂ H ₅	H	
15f	C ₆ H ₅		N	C	C ₂ H ₅	H	
15g	C ₆ H ₅		N	C	C ₂ H ₅	H	
15h	C ₆ H ₅		N	C	C ₂ H ₅	H	
15i	C ₆ H ₅		N	C	C ₂ H ₅	H	
15j	C ₆ H ₅		N	C	C ₂ H ₅	H	
15k	C ₆ H ₅		N	C	C ₂ H ₅	H	
15l	C ₆ H ₅		N	C	C ₂ H ₅	H	
16a	C ₆ H ₅		N	C	C ₂ H ₅	H	
16b	C ₆ H ₅		N	C	C ₂ H ₅	H	
16c	C ₆ H ₅		N	C	C ₂ H ₅	H	

Table 1 (continued)

Compd.	R ¹	M	X	Y	R ²	R ³	R ⁴
16d	C ₆ H ₅		N	C	C ₂ H ₅	H	
16e	C ₆ H ₅		N	C	C ₂ H ₅	H	
16f	C ₆ H ₅		N	C	C ₂ H ₅	H	
16g	C ₆ H ₅		N	C	C ₂ H ₅	H	
16h	C ₆ H ₅		N	C	C ₂ H ₅	H	
16i	C ₆ H ₅		N	C	C ₂ H ₅	H	
16j	C ₆ H ₅		N	C	C ₂ H ₅	H	
16k	C ₆ H ₅		N	C	C ₂ H ₅	H	
19a	CH ₃		N	C	C ₂ H ₅	H	
19b	C ₆ H ₅		N	C	C ₂ H ₅	H	
20a	CH ₃		N	C	C ₂ H ₅	H	
26a	CH ₃		C	N	H	C ₂ H ₅	
26b	C ₆ H ₅		C	N	H	C ₂ H ₅	
27a	CH ₃		C	N	H	C ₂ H ₅	
27b	C ₆ H ₅		C	N	H	C ₂ H ₅	

greatly favored compared to the C-5 positions.

To confirm that compounds exhibit anti-tumor activity through VDR, we used RNA interference (RNAi) in MCF-7 cells. As shown in Fig. 3, BrdU was employed, we found that silence the VDR abolished representative compounds induced anti-tumor activity. These data suggest that representative compounds exert their anti-tumor activity through VDR.

2.3. *In vitro* VDR binding affinity

In vitro receptor binding affinity of compounds for VDR was evaluated with VDR competitor assay and 1,25(OH)₂D₃ was used as the positive control. The target compounds were performed at a concentration of 1 μM and we defined VDR binding affinity of the 1,25(OH)₂D₃ as 100%, so the relative VDR binding affinity of testing compounds (%) = (mP_{DMSO} - mP_{Testing Compound})/(mP_{DMSO} - mP_{1,25(OH)₂D₃) × 100%, and the relative binding affinity are listed in Table 3. Replacing the 2'-OH group with sulfonyl group (15a) was generally well tolerated, with only slight changes in binding affinity being observed. By modifying the hydrophilic groups in the pyrrol part, change the chiral of α-position carbon atom to give (15c) resulted in the complete loss of VDR binding affinity. Similar detrimental effect was observed after its replacement the methyl group with large steric bulk groups (15d, 15e and 15f) as well as}

Table 2

In vitro antiproliferative activity of synthesized compounds against various human cancer cell lines.

Compd.	IC ₅₀ (μM) ^a		
	BXPC-3	MCF-7	PC-3
14a	17.92 ± 0.73	43.67 ± 0.63	NA ^b
14b	19.98 ± 0.18	NA	NA
14c	NA	NA	NA
14h	NA	NA	40.37 ± 2.82
14i	NA	NA	6.49 ± 0.15
14m	NA	NA	NA
14n	6.43 ± 0.19	6.47 ± 0.04	6.89 ± 0.36
14o	6.27 ± 0.04	4.68 ± 0.20	7.13 ± 0.39
15a	15.30 ± 6.16	10.78 ± 2.27	9.52 ± 0.66
15b	19.94 ± 0.05	15.47 ± 1.40	17.74 ± 1.57
15c	10.01 ± 0.30	10.63 ± 1.44	7.79 ± 0.28
15d	18.28 ± 0.89	20.65 ± 0.88	9.85 ± 0.69
15e	45.39 ± 1.67	28.84 ± 1.27	3.56 ± 0.19
15f	7.72 ± 0.85	25.47 ± 0.60	7.30 ± 0.19
15g	13.15 ± 0.76	18.82 ± 1.22	10.61 ± 0.58
15h	26.58 ± 1.70	41.95 ± 0.89	11.32 ± 0.69
15i	15.90 ± 0.75	28.52 ± 2.07	12.14 ± 0.95
15j	NA	27.42 ± 0.34	14.07 ± 0.47
15k	NA	31.37 ± 0.41	6.81 ± 0.76
15l	16.44 ± 0.74	29.57 ± 0.91	13.43 ± 0.96
16a	20.79 ± 1.03	35.47 ± 0.12	16.79 ± 0.78
16b	NA	33.08 ± 0.87	30.05 ± 1.17
16c	20.07 ± 0.88	NA	20.07 ± 0.26
16d	NA	41.19 ± 0.32	26.30 ± 0.20
16e	16.22 ± 0.20	24.46 ± 1.91	3.65 ± 0.30
16f	13.90 ± 0.66	44.71 ± 0.29	3.07 ± 0.79
16g	NA	NA	14.36 ± 0.56
16h	NA	NA	NA
16i	NA	NA	NA
16j	NA	NA	NA
16k	NA	NA	NA
19a	5.13 ± 0.35	5.16 ± 0.10	4.01 ± 0.80
19b	5.67 ± 0.40	4.90 ± 0.85	2.23 ± 0.14
20a	33.67 ± 1.24	14.72 ± 0.45	46.68 ± 0.12
26a	4.11 ± 0.34	4.64 ± 0.34	9.54 ± 0.38
26b	5.37 ± 0.35	4.70 ± 0.86	2.62 ± 0.21
27a	30.39 ± 0.71	16.29 ± 1.13	36.57 ± 0.02
27b	4.69 ± 0.61	2.03 ± 0.20	6.08 ± 0.89
sw-22	15.78 ± 1.58	18.23 ± 0.34	8.50 ± 0.02
1,25(OH) ₂ D ₃ ^c	21.07 ± 0.29	11.43 ± 0.32	9.53 ± 0.35

^a Results are expressed as the mean IC₅₀ of three experiments.

^b Not active (IC₅₀ > 50 μM).

^c 1,25(OH)₂D₃ was used as the positive control.

with hydroxyl contained alkyl groups (**15i**, **15k** and **15l**). As similar as SARs of the antiproliferative activity (section 2.2), compounds with the carboxyl acid and methyl ester groups at terminal of side chain show weak binding affinity. In contrast, *in vitro* VDR binding affinity recovered with the introduction of nitrogen atoms contained side chain (**14n**, **14o**). In particular, high activity was obtained with the *N,N*-diethylpropan-1-amine (**14o**) derivatives, showing 1.45-fold better VDR binding affinity than **sw-22**. Reduction of sulfonyl (**19b**) as well as replacement the phenyl adjacent sulfonyl with methyl group (**20a**) resulted in weakly active analogues. Interestingly, reduce the sulfonyl and replace the phenyl with methyl group simultaneously (**19a**), resulted in maintained binding affinity, which we postulate to be due to sulfur atom formed interaction with amino acid residues of the VDR LBD. Substitution at the C-4 position of pyrrole ring lead to an activity maintained compound **27b**.

Subsequently, we further evaluated the VDR binding affinities (IC₅₀) of compounds **19a** and **27b** with excellent relative VDR binding affinity at 1 μM, **sw-22** and 1,25(OH)₂D₃ were used as control. As shown in Fig. 4, compounds **19a** (IC₅₀ = 89.1 nM) and **27b** (IC₅₀ = 125.4 nM) shown maintained VDR binding affinity compare with the lead compound **sw-22** (IC₅₀ = 115.3 nM).

However, none of these compounds showed similar VDR binding affinity with the natural hormone 1,25(OH)₂D₃ (IC₅₀ = 1.42 nM). We hypothesized that the lower VDR binding affinity of phenylpyrrolyl pentane derivatives might result from less hydrogen bonds interaction with the ligand binding domain of VDR (VDR-LBD) than 1,25(OH)₂D₃.

2.4. Transactivation

To estimate agonistic properties of representative compounds [33], a transactivation assay in HEK293 cells was performed using pGL4.27-SPP × 3-Luc reporter plasmid as the VDRE activated reporter, pRL-TK as the internal reference and to normalize the expression of luciferase, pENTER-CMV-hVDR was to enhance the expression of VDR and pENTER-CMV-hRXRα expressing RXRα as the heterodimer partner of VDR. Representative compounds **19a** and **27b** were tested, **sw-22** and 1,25(OH)₂D₃ were used as positive control. As shown in Fig. 5, compounds **19a** and **27b** showed concentration-dependent transcriptional activity and acted as potent agonists. However, none of the compounds activated the reporter gene transcription better than positive controls 1,25(OH)₂D₃.

2.5. Molecular docking study

Docking studies were carried out to understand the atomic level interaction of **19a** and **27b** with VDR. The binding models of **19a** and **27b** with VDR-LBD (PDB ID: 2ZFX) were predicted and the most suitable conformations of the ligands were selected based on the calculated docking scores by means of the bonding strength. As shown in Fig. 6A, the oxygen atom on the sulfonyl group could form hydrogen bond with His393, the same interaction was found in lead compound **sw-22** [25], which support the hypothesis that the sulfonyl group on the side chain could mimic the function of 2'-OH group. And the heteroatom on amide bond could make interactions with Ser233 and Ser274. Besides, the sulfur atom at the side chain of **27b** formed the similar hydrogen bond with His393 and His301, and the N atom on amide bond could form hydrogen bond with Ser233 (Fig. 6B).

2.6. Cell cycle assay and cell apoptosis

Given the inhibitory effect of compounds **14n**, **14o**, **15a**, **15f**, **19a**, **19b**, **26a**, **26b** and **27b** on MCF-7 cells, we analyzed changes in cell cycle distribution and apoptosis in response to these representative compounds. Flow cytometry analysis of MCF-7 cells treated with representative compounds (1 μM) for 24 h revealed that compared with the control (49.3% of cells in G0/G1 phase), selected compounds induced cell cycle arrest at G0/G1 phase (Fig. 7A). Among them, the percentage of compounds **19a** and **27b** induced cells in G0/G1 phase was 55.3 and 56.0%, respectively (Fig. 7B). And silence the VDR abolished the cell cycle arrest effect induced by representative compounds, which suggest that **19a** and **27b** exert their cell cycle arrest effect through VDR. The results in Fig. 8 indicate that **19a** and **27b** induced apoptosis levels in MCF-7 cells by VDR.

There were many of anticancer mechanisms of VDR modulators, including cyclin-dependent kinase (CDK) inhibitors p21, p27 stimulation and pro-apoptotic gene Bax stimulation [7]. To determine if representative compounds stimulate the expression of p21, p27 and Bax, MCF-7 cells were treated with **14n**, **14o**, **15a**, **15f**, **19a**, **19b**, **26a**, **26b** and **27b** at the concentrations of 1 μM for 24 h, and the expression of p21, p27 and Bax were examined. As shown in Figure S1, compounds **19a** and **27b** significantly increased the expression of p21, p27 and Bax.

Table 3
The relative VDR binding affinity of all target compounds at 1 μ M.

Compd.	Relative VDR binding ability (%) ^a	Compd.	Relative VDR binding ability (%) ^a
14a	14	16a	43
14b	31	16b	78
14c	28	16c	51
14h	42	16d	5
14i	73	16e	–
14m	– ^b	16f	88
14n	65	16g	28
14o	80	16h	69
15a	54	16i	25
15b	83	16j	41
15c	–	16k	59
15d	14	19a	76
15e	–	19b	72
15f	–	20a	53
15g	42	26a	62
15h	71	26b	28
15i	23	27a	60
15j	67	27b	82
15k	42	sw-22	55
15l	–	1,25(OH) ₂ D ₃	100

^a Relative VDR binding affinity of testing compounds (%) = $(mP_{DMSO} - mP_{Testing\ Compound}) / (mP_{DMSO} - mP_{1,25(OH)_2D_3}) \times 100\%$.

^b Means no activity.

Table 4
In vitro metabolic stability and water solubility of selected compounds.^a

Compd.	Solubility (μ g/mL)	Rat Microsome Stability $t_{1/2}$ (min)
14n	65.0	34.91
14o	117.3	62.43
15a	35.7	43.76
15f	27.8	46.32
19a	74.6	57.26
19b	25.6	53.72
26a	198.2	48.13
26b	0.6	71.44
27b	85.3	59.23
sw-22	1.7	25.76

^a See Experimental Section for assay descriptions.

2.7. Physicochemical and pharmacokinetic properties of representative compounds

We evaluated the *in vitro* metabolic stability (rat microsomal) and water solubility of target compounds with significant anti-tumor activity and VDR binding affinity (Table 4). These data provide information to further guide lead optimization, with the ultimate goal of testing compounds in animals and identification of a preclinical candidate. We are targeting solubility of greater than 50 μ g/mL (in pH 7.4 buffer), and rat microsomal stability of approximately 60 min half life for compounds to be further evaluated *in vivo* [30]. As expected, the compound containing sulfonyl group (15a) versus compound without sulfonyl group (sw-22) had better stability ($t_{1/2}$ = 43.76 vs. 25.76 min) in rat microsomes. By modifying the hydrophilic groups in the pyrrol part, introduce *N,N*-diethylpropan-1-amine side chain result in compound 14o with desirable metabolic stability ($t_{1/2}$ = 62.43 min). And compounds 19a and 27b showed desirable metabolic stability ($t_{1/2}$ = 57.26 and 57.23 min) either. In addition, sulfonyl contained compound (15a) showed a 21-fold better solubility than the compound without sulfonyl (sw-22) in solubility assay (35.7 vs. 1.7 μ g/mL). Furthermore, compounds 14n, 14o, 19a, 26a and 27b showed excellent solubility with 65.0, 117.3, 74.6, 198.2 and 85.3 μ g/mL, respectively.

Consequently, we profiled the pharmacokinetic properties of our two most potent analogues, 19a and 27b, which showed

desirable metabolic stability and solubility, as well as excellent anti-tumor activity. As control, our lead compound sw-22 was selected, and the pharmacokinetic parameters were shown in Table 5. Introduction of the sulfonyl group led to a modification of the PK profile and we clearly saw an improvement in terms of half-lives and bioavailability. Compound 19a showed with bioavailability of 43.2% and $t_{1/2}$ value of 10.75 h after intraperitoneal administration. And compound 27b displayed with bioavailability of 40.3% and $t_{1/2}$ value of 7.65 h after intraperitoneal administration. Both of 19a and 27b possessed better pharmacokinetic properties than lead compound sw-22, whose bioavailability was 32.5% and $t_{1/2}$ value was 3.47 h after intraperitoneal administration. These results were in line with the trend we preconceived that compounds contained the sulfonyl group will possess better pharmacokinetic properties. In our another work, we improved pharmacokinetic properties with another approach. We modified the hydroxyl group on the side chain from secondary alcohol to tertiary alcohol, the steric hinerance around hydroxyl group was enhanced, which could delay the metabolish of the hydroxyl group on the side chain and lead to a longer $t_{1/2}$ value [31].

2.8. *In vivo* anticancer activity assay

On the basis of their potent antiproliferative effects, desirable physicochemical and pharmacokinetic properties, compounds 19a and 27b were selected for *in vivo* studies. Breast tumor mouse model was generated by orthotopic transplantation of human MCF-7 cells in athymic nude mice. Our lead compound sw-22 was selected as positive control. In addition, the natural VDR modulator 1,25(OH)₂D₃, which has been used in a number of animal models of cancer and clinical trials for cancer treatment (prostate cancer and breast cancer) [5,7], was selected as positive control either. As shown in Fig. 9A and B, 19a and 27b showed better antitumor efficacy compared with sw-22 or 1,25(OH)₂D₃. In addition, treated with compounds 19a and 27b did not affect mouse body weight (Fig. 9C), which indicated that the 19a and 27b have no apparent toxicity to mice during the period of cancer treatment.

We further determined the expression of p21, p27 and Bax *in vivo* by immunohistochemistry assay (Fig. 9D). Compared with control and 1,25(OH)₂D₃, there was a significantly increased

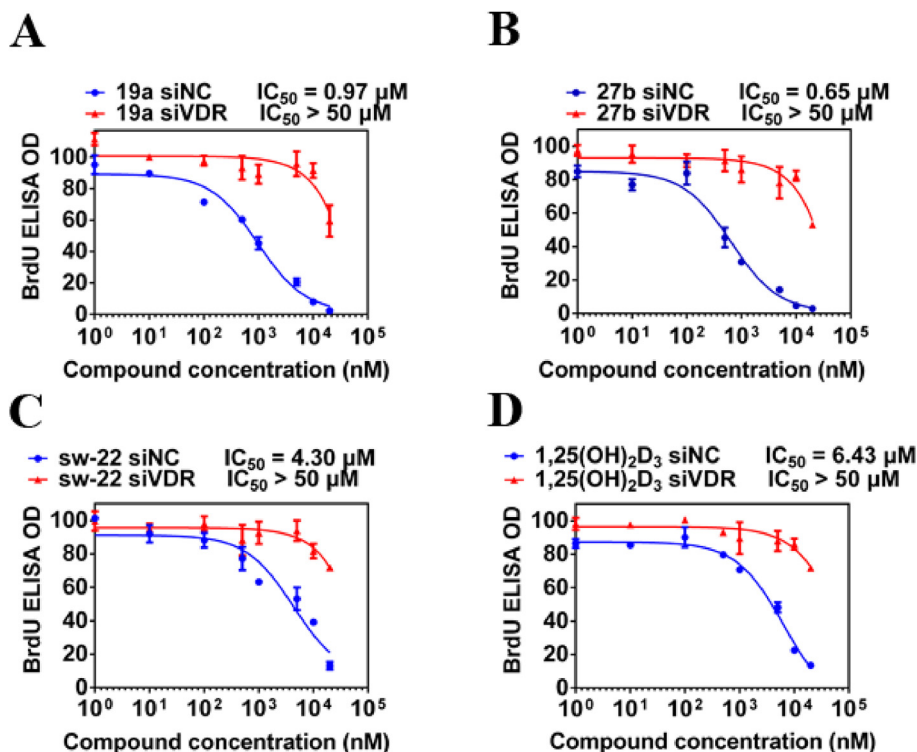


Fig. 3. Representative compounds inhibited the proliferation of MCF-7 cells through VDR. Negative control (siNC) or VDR-specific (siVDR) siRNA-transfected MCF-7 cells were treated with **19a**, **27b**, sw-22 and 1,25(OH)₂D₃ 16 h. BrdU incorporation was determined via a commercial available ELISA kit (Abcam). BrdU ELISA optical density (OD) at 450 nm was recorded. Dose-activity curves and IC₅₀ value are shown.(A, B, C and D).

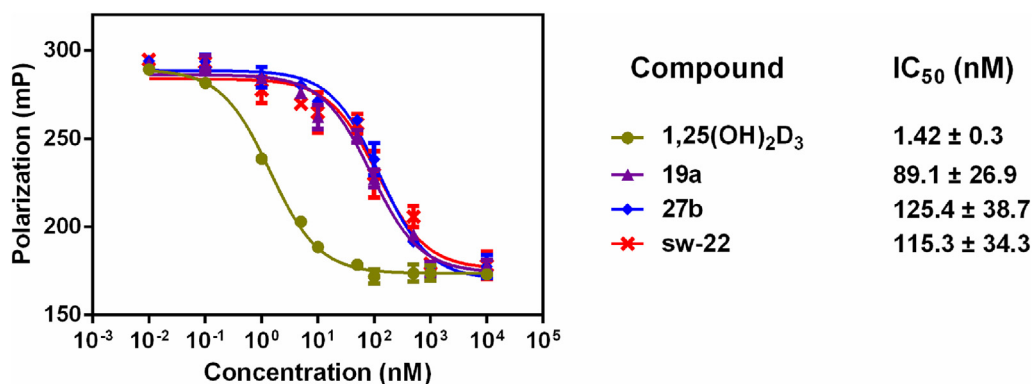


Fig. 4. The VDR ligand binding affinity of representative compounds. Fluorescence polarization competition assay was performed under equilibrium conditions *in vitro* and the competence of the Fluormone VDR Red ligand from the VDR-LBD by different compounds are shown (n = 3). (For interpretation of the references to color in this figure legend, the reader is referred to the Web version of this article.)

expression of p21, p27 and Bax in sections of the MCF-7 orthotopic tumors after they were treated with **19a** or **27b**. The results revealed that treatment with **19a** or **27b** dramatically increased the expression levels of the proapoptotic p21, p27 and Bax in MCF-7 cells, suggesting that **19a** or **27b** inhibited the tumor growth by inducing cell-cycle arrest.

2.9. *In vivo* calcemic activity assay

The level of serum calcium was measured to evaluate the safety profile of compounds **19a** and **27b**. 1,25(OH)₂D₃ and sw-22 were selected as the positive controls and vehicle as the negative control. As shown in Fig. 10, the serum calcium concentration of 1,25(OH)₂D₃ group was 0.31 μmol/mL before injection (day 7),

0.60 μmol/mL ongoing injection (day 17) and 0.61 μmol/mL after injection (day 27), indicating significant risk of hypercalcemia was induced by 1,25(OH)₂D₃. However, there was no significant change on serum calcium in mice when treated with compounds **19a** and **27b**. Therefore, compounds **19a** and **27b** had no hypercalcemia side effect *in vivo* at therapeutic doses.

3. Conclusions

On the basis of the potent non-secosteroidal VDR modulator reported by our group previously, we investigated the structure-activity and structure-property relationships around the 2'-hydroxyl group to improve the physicochemical properties, pharmacokinetic properties and anti-tumor activities. In this study, a new

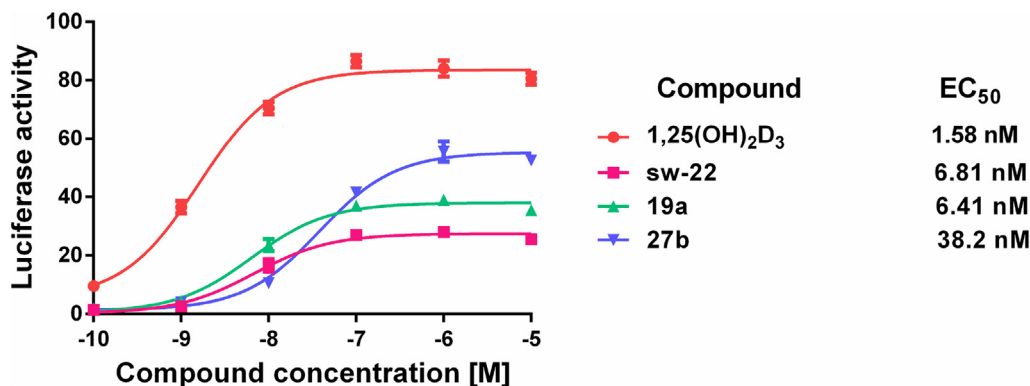


Fig. 5. Transcriptional activities of compounds were determined. HEK293 cells were cotransfected with TK-Spp × 3-LUC reporter plasmid, pRL-TK, pENTER-CMV-hRXR α and pENTER-CMV-hVDR. Eight hours after transfection, test compounds (**19a** and **27b**) and positive control (**sw-22** and 1,25(OH)₂D₃) were added. Luciferase activity assay was performed 24 h later using the Dual-Luciferase Assay System. Firefly luciferase activity was normalized to the corresponding Renilla luciferase activity. Data are shown as means \pm SD. * $P < 0.05$ vs. DMSO. All the experiments were performed three times.

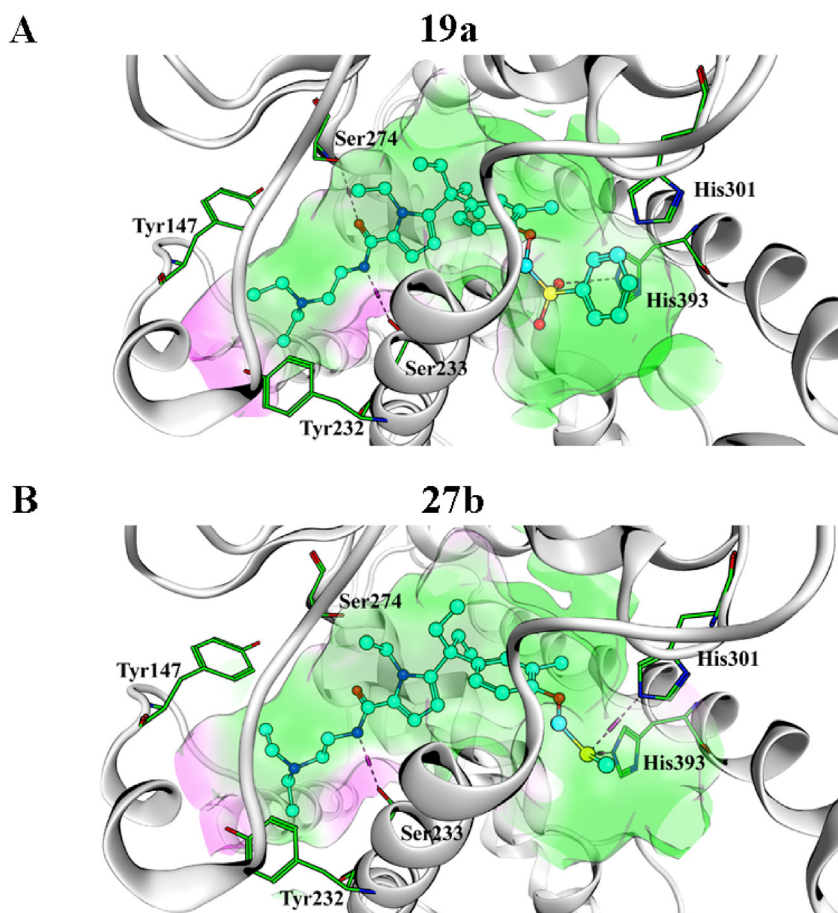


Fig. 6. The predicted binding model of **19a** (A) and **27b** (B). VDR-LBD of PDB reference 2ZFX is applied for molecular docking using Glide 5.5 in Schrödinger (2009). The most suitable conformations of the ligands were selected based on the calculated docking scores by means of the bonding strength. (A) Oxygen atom on the sulfonyl group at the side chain of compound **19a** was able to form hydrogen bond with the His393 of VDR-LBD. On the other side of the structure, the heteroatom on amide bond could make interactions with Ser233 and Ser274. (B) Sulfur atom at the side chain of **27b** formed the similar hydrogen bond with His393 and His301, and the N atom on amide bond could form hydrogen bond with Ser233.

series of sulfonyl-containing phenyl-pyrrolyl pentane analogues were synthesized. Screening assays of these derivatives identified compounds **19a** and **27b** as potential anti-tumor agents. Novel compounds **19a** and **27b**, feature sulfonyl groups on the side chain, are particularly attractive for future studies because of the following features: (i) Inhibition of cell proliferation with a low IC₅₀

via the arrest of cell cycle and induction of apoptosis by stimulating the expression of p21, p27 and Bax. (ii) The desirable drug-like properties including metabolic stability, water solubility and pharmacokinetic profiles that are crucial for compounds to exert activity *in vivo*. (iii) The excellent *in vivo* anti-tumor activity without hypercalcemia side effect. In summary, the favorable

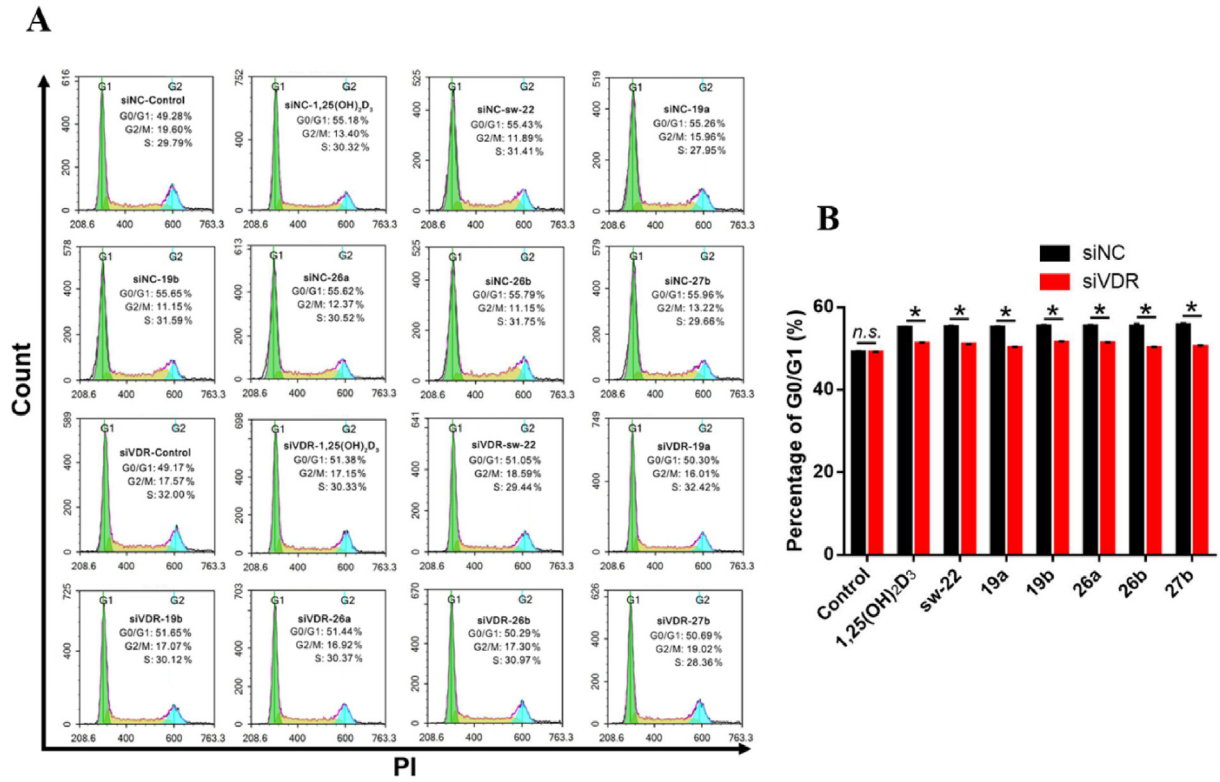


Fig. 7. Effects of representative compounds arrested the cell cycle in Negative control (siNC) or VDR-specific (siVDR) siRNA-transfected MCF-7 cells. (A) Flow cytometry analysis of cell cycle populations after treatment with 1 μ M compounds for 24 h. (B) The fold differences of cell population in the G0/G1 phase of the cell cycle after treatment of each compound. Data are shown as means \pm SD. * P < 0.05 vs. Control. All the experiments were performed three times.

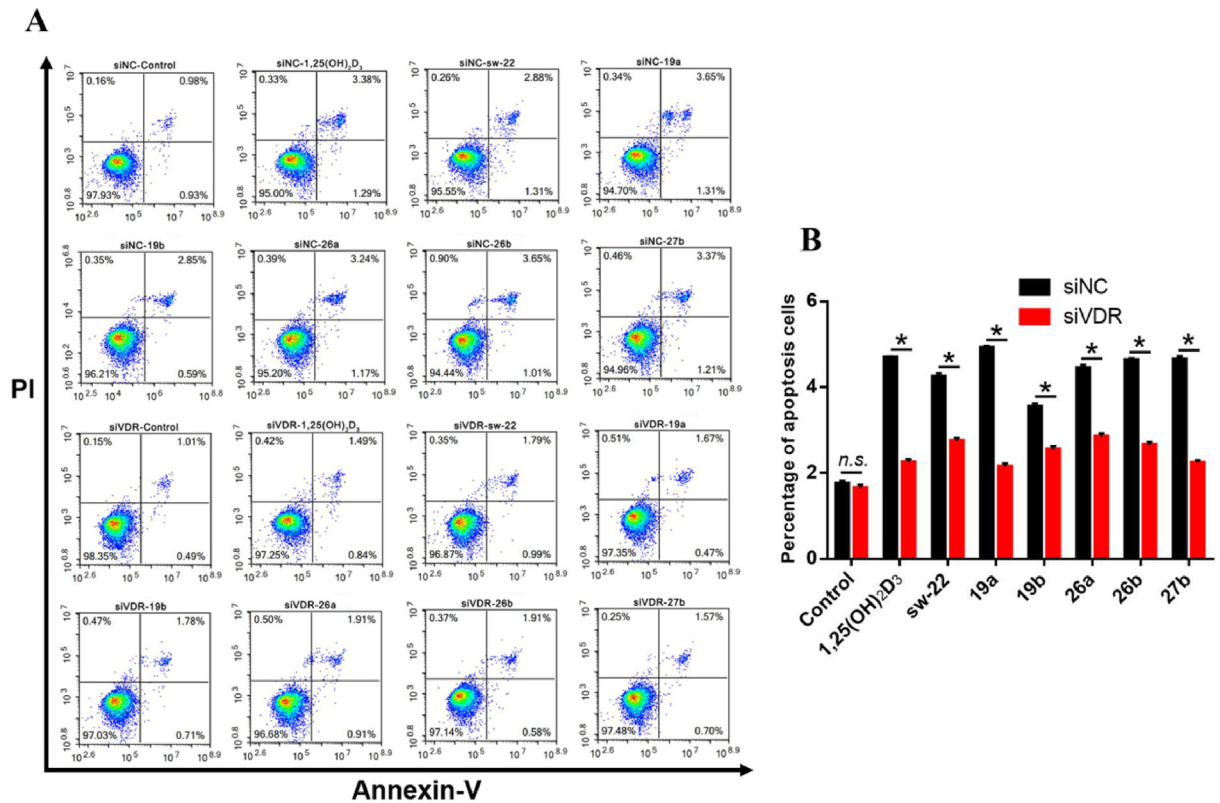


Fig. 8. Effects of representative compounds induced apoptosis in Negative control (siNC) or VDR-specific (siVDR) siRNA-transfected MCF-7 cells. (A) Flow cytometry analysis of apoptosis. Cells were exposed to 1 μ M compounds for 24 h. Cells were collected and stained with Annexin V-fluorescein isothiocyanate (FITC) and PI. (B) The fold differences of apoptotic quantification after exposure to each compound for 24 h. Data are shown as means \pm SD. * P < 0.05 vs. Control. All the experiments were performed three times.

Table 5
Pharmacokinetic Parameters of compounds **19a**, **27b** and **sw-22** in rats ^a.

Parameters	sw-22		19a		27b	
	i.v.	i.p.	i.v.	i.p.	i.v.	i.p.
	5 mg/kg	20 mg/kg	5 mg/kg	20 mg/kg	5 mg/kg	20 mg/kg
AUC(mg/L ^h)	4.65 ± 0.07	6.04 ± 0.23	11.79 ± 0.34	20.37 ± 3.54	7.47 ± 0.43	12.04 ± 0.19
t _{1/2} (h)	2.89 ± 0.12	3.47 ± 0.18	4.72 ± 0.21	10.75 ± 0.07	6.6 ± 0.25	7.65 ± 0.06
MRT(h)	5.54 ± 0.13	5.5 ± 0.24	8.08 ± 0.3	15.67 ± 0.02	9.72 ± 0.27	11.87 ± 0.11
CL (L/h)	1.08 ± 0.02	3.31 ± 0.13	0.42 ± 0.01	0.99 ± 0.17	0.67 ± 0.04	1.66 ± 0.02
F	—	32.47%	—	43.19%	—	40.29%

^a SD rats (male, 3 animals per group) weighted 180–220 g were used for the study (n = 3). Data were presented as Mean ± SD.

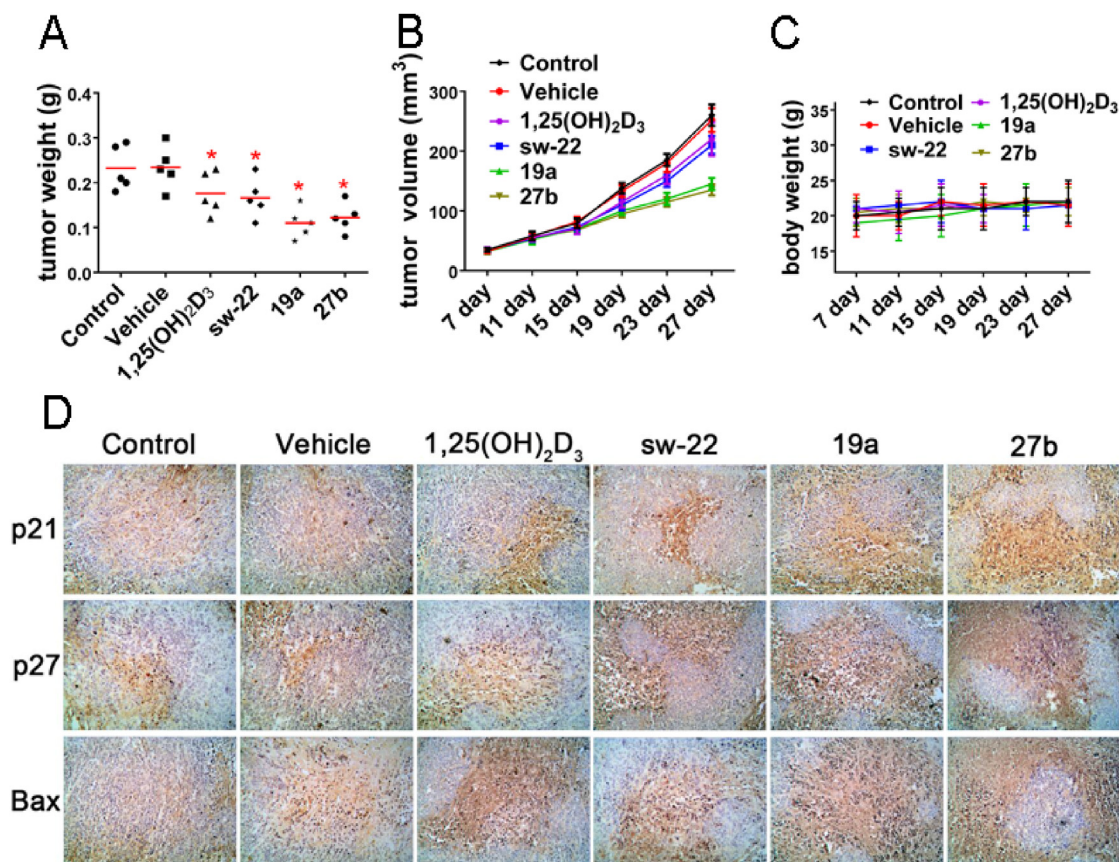


Fig. 9. Compounds **19a** and **27b** exert antitumor efficiency *in vivo*. (A) Differences in tumor weight in mice treated with vehicle, **19a**, **27b**, **sw-22** and 1,25(OH)₂D₃. **P* < 0.05 compared to the placebo group. (B) Differences in tumor size in mice exposed to vehicle, **19a**, **27b**, **sw-22** and 1,25(OH)₂D₃. (C) Changes in body weight of mice treated with vehicle, **19a**, **27b**, **sw-22** and 1,25(OH)₂D₃. (D) Expression of p21, p27 and Bax in the tumor sections of MCF-7-bearing mice was examined by immunohistochemistry (× 200).

physicochemical properties, pharmacokinetic properties and anti-tumor activity of **19a** and **27b** highlight their potential therapeutic applications in cancer treatment.

4. Experiment section

4.1. General materials and methods

All material and reagents were purchased from commercial sources and, unless otherwise stated, were used without further purification. High-resolution mass spectra (HRMS) were recorded on QSTAR XL Hybrid MS/MS mass spectrometer. ¹H NMR and ¹³C NMR were recorded employing Bruker AV-300 or AV-500 instruments using CDCl₃. Chemical shifts were given as δ (ppm) units relative to the internal standard tetramethylsilane (TMS). Column

chromatography separations were progressed on silica gel (200–300 mesh).

4.2. General procedure 1 - synthesis of compounds **14a-o**

To a solution of compound **13** (0.15 g, 0.32 mmol) in dichloromethane (50 mL), 3-(ethyliminomethylideneamino)-*N,N*-dimethylpropan-1-amine, hydrochloride (74.38 mg, 0.48 mmol), 1-Hydroxybenzotriazole (64.74 mg, 0.48 mmol) and triethylamine (48.49 mg, 0.48 mmol) was added at 0 °C. After stirring for 0.5 h, appropriate amine (0.48 mmol) was added. The reaction mixture was stirred at room temperature for 12 h and then H₂O (100 mL) was added. The organic phase were washed with brine and dried over anhydrous Na₂SO₄, filtered and concentrated. The residue was purified by silica gel column chromatography eluting with

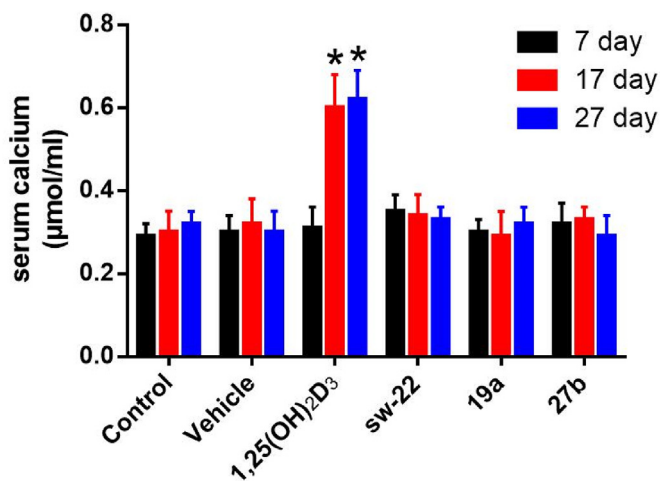


Fig. 10. (A) *In vivo* hypercalcemic effects of compounds **19a**, **27b**, **sw-22** and **1,25(OH)₂D₃** in the MCF-7 tumor-bearing mice. The venous blood were withdrawn before injection (day 7), ongoing injection (day 17) and after injection (day 27). The total calcium ion concentration was determined by calcium assay kit. Data are shown as means \pm SD. * $P < 0.05$ vs. Control.

appropriate mixture as indicated in each case.

4.2.1. Methyl (1-ethyl-5-(3-(3-methyl-4-((phenylsulfonyl)methoxy)phenyl)pentan-3-yl)-1H-pyrrole-2-carbonyl)-L-alaninate (**14a**)

Petroleum ether/ethyl acetate (25/1). Colorless oil. 87% yield. ¹H NMR (300 MHz, CDCl₃) δ (ppm) 7.98 (d, $J = 7.2$ Hz, 2H), 7.67 (t, $J = 7.3$ Hz, 1H), 7.55 (t, $J = 7.3$ Hz, 2H), 6.84 (d, $J = 8.5$ Hz, 1H), 6.81 (s, 1H), 6.67 (d, $J = 8.5$ Hz, 1H), 6.62 (d, $J = 4.0$ Hz, 1H), 6.16 (d, $J = 4.0$ Hz, 1H), 5.03 (s, 2H), 4.66–4.59 (m, 1H), 3.85–3.68 (m, 2H), 3.75 (s, 3H), 2.05 (s, 3H), 2.01–1.91 (m, 4H), 1.45 (d, $J = 7.1$ Hz, 3H), 0.79 (t, $J = 6.9$ Hz, 3H), 0.56 (t, $J = 7.3$ Hz, 6H). ¹³C NMR (75 MHz, CDCl₃) δ (ppm) 173.40, 161.14, 152.88, 143.09, 140.39, 136.63, 133.81, 129.55, 128.70, 128.60, 126.35, 124.93, 124.49, 111.53, 111.30, 107.82, 82.54, 51.89, 47.38, 45.96, 40.33, 27.95, 18.11, 15.88, 15.51, 7.65. ESI-HRMS calcd for C₃₀H₃₈N₂O₆S [M+Na]⁺ 577.2451, found 577.2355.

4.2.2. Methyl (1-ethyl-5-(3-(3-methyl-4-((phenylsulfonyl)methoxy)phenyl)pentan-3-yl)-1H-pyrrole-2-carbonyl)glycinate (**14b**)

Petroleum ether/ethyl acetate (30/1). Colorless oil. 79% yield. ¹H NMR (300 MHz, CDCl₃) δ (ppm) 7.98 (d, $J = 7.2$ Hz, 2H), 7.67 (t, $J = 7.3$ Hz, 1H), 7.56 (t, $J = 7.3$ Hz, 2H), 6.86–6.81 (m, 2H), 6.68 (d, $J = 8.5$ Hz, 1H), 6.63 (d, $J = 4.0$ Hz, 1H), 6.16 (d, $J = 4.0$ Hz, 1H), 5.03 (s, 2H), 4.11 (d, $J = 4.8$ Hz, 2H), 3.80 (q, $J = 7.0$ Hz, 2H), 3.76 (s, 3H), 2.06 (s, 3H), 2.04–1.89 (m, 4H), 0.81 (t, $J = 7.0$ Hz, 3H), 0.57 (t, $J = 7.3$ Hz, 6H). ¹³C NMR (75 MHz, CDCl₃) δ (ppm) 170.35, 152.88, 143.24, 140.37, 136.63, 133.82, 129.55, 128.71, 128.60, 126.36, 124.93, 111.53, 107.92, 82.54, 51.80, 45.97, 40.64, 40.37, 27.95, 15.88, 15.53, 7.66. ESI-HRMS calcd for C₂₉H₃₆N₂O₆S [M+Na]⁺ 563.2294, found 563.2195.

4.2.3. Methyl (1-ethyl-5-(3-(3-methyl-4-((phenylsulfonyl)methoxy)phenyl)pentan-3-yl)-1H-pyrrole-2-carbonyl)-D-alaninate (**14c**)

Petroleum ether/ethyl acetate (30/1). Colorless oil. 83% yield. ¹H NMR (300 MHz, CDCl₃) δ (ppm) 7.98 (d, $J = 7.2$ Hz, 2H), 7.67 (t, $J = 7.3$ Hz, $J = 1.3$ Hz, 1H), 7.55 (t, $J = 7.3$ Hz, 2H), 6.85–6.81 (m, 2H), 6.67 (d, $J = 8.5$ Hz, 1H), 6.62 (d, $J = 4.0$ Hz, 1H), 6.15 (d, $J = 4.0$ Hz, 1H), 5.03 (s, 2H), 4.69–4.59 (m, 1H), 3.85–3.68 (m, 2H), 3.75 (s, 3H), 2.06 (s, 3H), 2.03–1.91 (m, 4H), 1.45 (d, $J = 7.2$ Hz, 3H), 0.79 (t, $J = 6.9$ Hz, 3H), 0.56 (t, $J = 7.3$ Hz, 6H). ¹³C NMR (75 MHz, CDCl₃) δ (ppm) 173.83, 161.58, 153.30, 143.52, 140.82, 137.06, 134.24, 129.98, 129.13, 129.03, 126.78, 125.36, 124.92, 111.97, 111.74, 108.25,

82.97, 52.31, 47.81, 46.39, 40.76, 29.62, 28.39, 18.53, 16.30, 15.94, 8.09. ESI-HRMS calcd for C₃₀H₃₈N₂O₆S [M+Na]⁺ 577.2451, found 577.2363.

4.2.4. Methyl 3-(1-ethyl-5-(3-(3-methyl-4-((phenylsulfonyl)methoxy)phenyl)pentan-3-yl)-1H-pyrrole-2-carboxamido)propanoate (**14h**)

Petroleum ether/ethyl acetate (30/1). Colorless oil. 69% yield. ¹H NMR (300 MHz, CDCl₃) δ (ppm) 7.97 (d, $J = 7.3$ Hz, 2H), 7.67 (tt, $J = 7.3$ Hz, $J = 1.3$ Hz, 1H), 7.55 (t, $J = 7.3$ Hz, 2H), 6.84–6.81 (m, 2H), 6.67 (d, $J = 8.7$ Hz, 1H), 6.51 (d, $J = 4.0$ Hz, 1H), 6.13 (d, $J = 4.0$ Hz, 1H), 5.03 (s, 2H), 3.80 (q, $J = 6.9$ Hz, 2H), 3.69 (s, 3H), 3.59 (d, $J = 6.0$ Hz, 2H), 2.58 (t, $J = 6.0$ Hz, 2H), 2.05 (s, 3H), 2.03–1.90 (m, 4H), 0.79 (t, $J = 6.9$ Hz, 3H), 0.55 (t, $J = 7.3$ Hz, 6H). ¹³C NMR (75 MHz, CDCl₃) δ (ppm) 173.10, 162.08, 153.29, 143.20, 140.87, 137.06, 134.23, 129.96, 129.12, 129.02, 126.75, 125.37, 111.96, 111.21, 108.12, 82.97, 51.69, 46.37, 40.74, 34.59, 34.03, 30.17, 28.37, 16.29, 15.99, 8.08, 0.94. ESI-HRMS calcd for C₃₀H₃₈N₂O₆S [M+Na]⁺ 577.2451, found 577.2356.

4.2.5. Dimethyl (1-ethyl-5-(3-(3-methyl-4-((phenylsulfonyl)methoxy)phenyl)pentan-3-yl)-1H-pyrrole-2-carbonyl)-L-aspartate (**14i**)

Petroleum ether/ethyl acetate (20/1). Colorless oil. 72% yield. ¹H NMR (300 MHz, CDCl₃) δ (ppm) 7.97 (d, $J = 7.3$ Hz, 2H), 7.67 (tt, $J = 7.3$ Hz, $J = 1.3$ Hz, 1H), 7.55 (tt, $J = 7.3$ Hz, $J = 1.3$ Hz, 2H), 6.84–6.81 (m, 3H), 6.64 (d, $J = 4.0$ Hz, 1H), 6.16 (d, $J = 4.0$ Hz, 1H), 5.03 (s, 2H), 4.96–4.90 (m, 1H), 3.83–3.77 (m, 2H), 3.75 (s, 3H), 3.69 (s, 3H), 3.10–3.03 (m, 1H), 2.91–2.84 (m, 1H), 2.06 (s, 3H), 2.04–1.91 (m, 4H), 0.79 (t, $J = 6.9$ Hz, 3H), 0.56 (t, $J = 7.3$ Hz, 6H). ¹³C NMR (75 MHz, CDCl₃) δ (ppm) 171.57, 171.54, 161.55, 153.32, 143.80, 140.77, 137.07, 134.24, 129.97, 129.13, 129.02, 126.79, 125.37, 124.65, 112.21, 111.98, 108.38, 82.96, 52.67, 51.94, 48.26, 46.40, 40.81, 36.31, 28.38, 16.30, 15.92, 8.08. ESI-HRMS calcd for C₃₂H₄₀N₂O₈S [M+Na]⁺ 635.2505, found 635.2414.

4.2.6. Tert-butyl (2-(1-ethyl-5-(3-(3-methyl-4-((phenylsulfonyl)methoxy)phenyl)pentan-3-yl)-1H-pyrrole-2-carboxamido)ethyl)carbamate (**14m**)

Petroleum ether/ethyl acetate (20/1). Colorless oil. 76% yield. ¹H NMR (300 MHz, CDCl₃) δ (ppm) 7.97 (d, $J = 7.2$ Hz, 2H), 7.66 (tt, $J = 7.4$ Hz, $J = 1.3$ Hz, 1H), 7.55 (t, $J = 7.4$ Hz, 2H), 6.85–6.80 (m, 2H), 6.67 (d, $J = 8.5$ Hz, 1H), 6.57 (d, $J = 4.0$ Hz, 1H), 6.14 (d, $J = 4.0$ Hz, 1H), 5.03 (s, 2H), 3.82 (q, $J = 7.1$ Hz, 2H), 3.43 (t, $J = 5.3$ Hz, 2H), 3.30 (t, $J = 5.3$ Hz, 2H), 2.05 (s, 3H), 2.01–1.90 (m, 4H), 1.41 (s, 9H), 0.80 (t, $J = 7.0$ Hz, 3H), 0.56 (t, $J = 7.1$ Hz, 6H). ¹³C NMR (75 MHz, CDCl₃) δ (ppm) 162.35, 152.85, 142.73, 140.49, 136.62, 133.80, 129.55, 128.69, 128.59, 126.31, 124.93, 124.75, 111.51, 111.03, 107.78, 82.54, 45.94, 40.32, 40.15, 39.82, 27.89, 15.86, 15.60, 7.65. ESI-HRMS calcd for C₃₃H₄₅N₃O₆S [M+Na]⁺ 634.3029, found 634.2902.

4.2.7. N-(2-aminoethyl)-1-ethyl-5-(3-(3-methyl-4-((phenylsulfonyl)methoxy)phenyl)pentan-3-yl)-1H-pyrrole-2-carboxamide (**14n**)

Dichloromethane/methanol (15/1). Colorless oil. 41% yield. ¹H NMR (300 MHz, CDCl₃) δ (ppm) 7.96 (d, $J = 7.2$ Hz, 2H), 7.66 (tt, $J = 7.4$ Hz, $J = 1.3$ Hz, 1H), 7.55 (t, $J = 7.4$ Hz, 2H), 6.83–6.80 (m, 2H), 6.67–6.66 (m, 2H), 6.13 (d, $J = 4.0$ Hz, 1H), 5.03 (s, 2H), 3.79 (q, $J = 6.7$ Hz, 2H), 3.44 (q, $J = 5.7$ Hz, 2H), 2.94 (t, $J = 5.7$ Hz, 2H), 2.05 (s, 3H), 2.00–1.89 (m, 4H), 1.41 (s, 9H), 0.79 (t, $J = 6.9$ Hz, 3H), 0.55 (t, $J = 7.1$ Hz, 6H). ¹³C NMR (75 MHz, CDCl₃) δ (ppm) 162.88, 153.31, 143.54, 140.85, 137.07, 134.28, 129.88, 129.17, 129.04, 126.71, 125.49, 124.89, 119.55, 112.41, 112.12, 108.48, 82.97, 46.42, 41.10, 40.86, 39.41, 29.66, 28.40, 16.34, 16.12, 8.14, 0.98. ESI-HRMS calcd for C₂₈H₃₇N₃O₄S [M+H]⁺ 512.2505, found 512.2589.

4.2.8. *N*-(2-(diethylamino)ethyl)-1-ethyl-5-(3-(3-methyl-4-((phenylsulfonyl)methoxy)phenyl)pentan-3-yl)-1H-pyrrole-2-carboxamide (**14o**)

Dichloromethane/methanol (30/1). Colorless oil. 81% yield. ¹H NMR (300 MHz, CDCl₃) δ (ppm) 7.98 (d, *J* = 7.2 Hz, 2H), 7.67 (t, *J* = 7.4 Hz, 1H), 7.56 (t, *J* = 7.4 Hz, 2H), 6.86–6.82 (m, 2H), 6.72–6.65 (m, 2H), 6.15 (d, *J* = 4.0 Hz, 1H), 5.03 (s, 2H), 3.82 (q, *J* = 7.1 Hz, 2H), 3.49 (q, *J* = 5.5 Hz, 2H), 2.77–2.70 (m, 6H), 2.06 (s, 3H), 2.02–1.93 (m, 4H), 1.16 (t, *J* = 7.1 Hz, 6H), 0.80 (t, *J* = 6.9 Hz, 3H), 0.56 (t, *J* = 7.3 Hz, 6H). ¹³C NMR (75 MHz, CDCl₃) δ (ppm) 140.58, 133.80, 129.58, 128.69, 128.60, 124.96, 111.50, 107.90, 82.56, 51.88, 46.97, 45.95, 40.30, 35.62, 27.96, 15.86, 15.63, 10.37, 7.66. ESI-HRMS calcd for C₃₂H₄₅N₃O₄S [M+H]⁺ 568.3131, found 568.3249.

4.3. General procedure 2 - synthesis of compounds **15a–l**

To a solution of appropriate ester **14a–14l** (0.33 mmol) in methanol (20 mL), NaBH₄ (31.40 mg, 0.83 mmol) was added portionwise at 0 °C. The reaction mixture was stirred at 25 °C for 8 h and the solution was evaporated. Then H₂O (20 mL) and EtOAc (50 mL) was added and the organic phase were washed with brine and dried over anhydrous Na₂SO₄, filtered and concentrated. The residue was purified by silica gel column chromatography eluting with appropriate mixture as indicated in each case.

4.3.1. *(S)*-1-ethyl-*N*-(1-hydroxypropan-2-yl)-5-(3-(3-methyl-4-((phenylsulfonyl)methoxy)phenyl)pentan-3-yl)-1H-pyrrole-2-carboxamide (**15a**)

Petroleum ether/ethyl acetate (5/1). oil. 81% yield. ¹H NMR (300 MHz, CDCl₃) δ (ppm) 7.98 (d, *J* = 7.2 Hz, 2H), 7.67 (t, *J* = 7.3 Hz, 1H), 7.56 (t, *J* = 7.3 Hz, 2H), 6.85–6.81 (m, 2H), 6.69 (d, *J* = 8.2 Hz, 1H), 6.56 (d, *J* = 4.0 Hz, 1H), 6.14 (d, *J* = 4.0 Hz, 1H), 5.03 (s, 2H), 4.16–4.10 (m, 1H), 3.88–3.74 (m, 2H), 3.72–3.53 (m, 2H), 2.06 (s, 3H), 2.01–1.91 (m, 4H), 1.22 (d, *J* = 6.8 Hz, 3H), 0.80 (t, *J* = 6.9 Hz, 3H), 0.57 (t, *J* = 7.3 Hz, 6H). ¹³C NMR (75 MHz, CDCl₃) δ (ppm) 162.63, 152.88, 143.14, 140.37, 133.82, 129.52, 128.71, 128.59, 126.35, 124.93, 111.56, 111.04, 107.77, 82.54, 67.36, 47.36, 45.97, 40.33, 27.95, 16.70, 15.88, 15.58, 7.66. ESI-HRMS calcd for C₂₉H₃₈N₂O₅S [M+Na]⁺ 549.2501, found 549.2409.

4.3.2. 1-ethyl-*N*-(2-hydroxyethyl)-5-(3-(3-methyl-4-((phenylsulfonyl)methoxy)phenyl)pentan-3-yl)-1H-pyrrole-2-carboxamide (**15b**)

Petroleum ether/ethyl acetate (5/1). oil. 77% yield. ¹H NMR (300 MHz, CDCl₃) δ (ppm) 7.98 (d, *J* = 7.3 Hz, 2H), 7.67 (tt, *J* = 7.4 Hz, 1H), 7.56 (t, *J* = 7.4 Hz, 2H), 6.85–6.81 (m, 2H), 6.68 (d, *J* = 8.4 Hz, 1H), 6.57 (d, *J* = 4.0 Hz, 1H), 6.15 (d, *J* = 4.0 Hz, 1H), 5.03 (s, 2H), 3.80 (q, *J* = 7.0 Hz, 2H), 3.76 (t, *J* = 5.0 Hz, 2H), 3.50 (t, *J* = 5.0 Hz, 2H), 2.06 (s, 3H), 2.04–1.92 (m, 4H), 0.81 (t, *J* = 7.0 Hz, 3H), 0.57 (t, *J* = 7.3 Hz, 6H). ¹³C NMR (75 MHz, DMSO) δ (ppm) 163.07, 152.89, 143.16, 140.37, 136.61, 133.82, 129.52, 128.71, 128.59, 126.36, 124.93, 124.55, 111.56, 111.17, 107.85, 82.54, 62.61, 45.98, 42.06, 40.37, 29.19, 27.95, 15.89, 15.59, 7.66. ESI-HRMS calcd for C₂₈H₃₆N₂O₅S [M+Na]⁺ 535.2345, found 535.2283.

4.3.3. *(R)*-1-ethyl-*N*-(1-hydroxypropan-2-yl)-5-(3-(3-methyl-4-((phenylsulfonyl)methoxy)phenyl)pentan-3-yl)-1H-pyrrole-2-carboxamide (**15c**)

Petroleum ether/ethyl acetate (3/1). oil. 65% yield. ¹H NMR (300 MHz, CDCl₃) δ (ppm) 7.97 (d, *J* = 7.2 Hz, 2H), 7.67 (t, *J* = 7.3 Hz, 1H), 7.56 (t, *J* = 7.3 Hz, 2H), 6.85–6.81 (m, 2H), 6.68 (d, *J* = 8.2 Hz, 1H), 6.56 (d, *J* = 4.0 Hz, 1H), 6.14 (d, *J* = 4.0 Hz, 1H), 5.03 (s, 2H), 4.16–4.10 (m, 1H), 3.88–3.71 (m, 2H), 3.71–3.53 (m, 2H), 2.06 (s, 3H), 2.01–1.91 (m, 4H), 1.22 (d, *J* = 6.8 Hz, 3H), 0.80 (t, *J* = 6.9 Hz, 3H), 0.56 (t, *J* = 7.3 Hz, 6H). ¹³C NMR (75 MHz, CDCl₃) δ (ppm)

163.07, 153.32, 143.61, 140.79, 137.06, 134.25, 129.95, 129.14, 129.03, 126.79, 125.36, 125.09, 114.53, 111.99, 111.53, 108.22, 82.98, 67.81, 47.84, 46.41, 40.77, 28.38, 17.13, 16.31, 16.01, 8.09. ESI-HRMS calcd for C₂₉H₃₈N₂O₅S [M+Na]⁺ 549.2501, found 549.2383.

4.3.4. 1-ethyl-*N*-(1-hydroxy-2-methylpropan-2-yl)-5-(3-(3-methyl-4-((phenylsulfonyl)methoxy)phenyl)pentan-3-yl)-1H-pyrrole-2-carboxamide (**15d**)

Petroleum ether/ethyl acetate (4/1). oil. 68% yield. ¹H NMR (300 MHz, CDCl₃) δ (ppm) 7.97 (d, *J* = 7.3 Hz, 2H), 7.67 (tt, *J* = 7.3 Hz, *J* = 1.3 Hz, 1H), 7.56 (t, *J* = 7.3 Hz, 2H), 6.85–6.81 (m, 2H), 6.69 (d, *J* = 8.7 Hz, 1H), 6.49 (d, *J* = 4.0 Hz, 1H), 6.13 (d, *J* = 4.0 Hz, 1H), 5.03 (s, 2H), 3.77 (q, *J* = 7.0 Hz, 2H), 3.61 (s, 2H), 2.06 (s, 3H), 2.03–1.90 (m, 4H), 1.33 (s, 6H), 0.77 (t, *J* = 7.0 Hz, 3H), 0.56 (t, *J* = 7.3 Hz, 6H). ¹³C NMR (75 MHz, CDCl₃) δ (ppm) 163.48, 153.34, 143.60, 140.76, 137.08, 134.27, 130.02, 129.93, 129.15, 129.03, 126.80, 125.64, 125.39, 112.04, 111.98, 111.50, 108.05, 107.32, 82.98, 71.20, 56.10, 46.41, 40.61, 39.76, 29.64, 28.41, 24.81, 16.33, 15.96, 8.17, 8.10. ESI-HRMS calcd for C₃₀H₄₀N₂O₅S [M+Na]⁺ 563.2658, found 563.2558.

4.3.5. 1-ethyl-*N*-(1-(hydroxymethyl)cyclopropyl)-5-(3-(3-methyl-4-((phenylsulfonyl)methoxy)phenyl)pentan-3-yl)-1H-pyrrole-2-carboxamide (**15e**)

Petroleum ether/ethyl acetate (5/1). oil. 79% yield. ¹H NMR (300 MHz, CDCl₃) δ (ppm) 7.97 (d, *J* = 7.4 Hz, 2H), 7.67 (t, *J* = 7.4 Hz, 1H), 7.55 (t, *J* = 7.7 Hz, 2H), 6.83–6.79 (m, 2H), 6.68 (d, *J* = 8.6 Hz, 1H), 6.51 (d, *J* = 4.0 Hz, 1H), 6.13 (d, *J* = 4.0 Hz, 1H), 5.03 (s, 2H), 3.78 (q, *J* = 6.9 Hz, 2H), 3.61 (s, 3H), 2.05 (s, 3H), 2.02–1.90 (m, 4H), 0.95–0.91 (m, 2H), 0.87–0.84 (m, 2H), 0.81 (t, *J* = 6.9 Hz, 3H), 0.55 (t, *J* = 7.3 Hz, 6H). ¹³C NMR (75 MHz, CDCl₃) δ (ppm) 164.79, 153.34, 144.08, 140.67, 137.03, 134.27, 129.91, 129.15, 129.01, 126.81, 125.35, 124.54, 112.02, 108.36, 82.96, 70.01, 46.43, 40.85, 35.26, 30.27, 29.62, 28.37, 16.32, 16.00, 13.02, 8.08. ESI-HRMS calcd for C₃₀H₃₈N₂O₅S [M+Na]⁺ 561.2501, found 561.2400.

4.3.6. *(S)*-1-ethyl-*N*-(1-hydroxy-3-methylbutan-2-yl)-5-(3-(3-methyl-4-((phenylsulfonyl)methoxy)phenyl)pentan-3-yl)-1H-pyrrole-2-carboxamide (**15f**)

Petroleum ether/ethyl acetate (5/1). oil. 80% yield. ¹H NMR (300 MHz, CDCl₃) δ (ppm) 7.95 (d, *J* = 7.2 Hz, 2H), 7.65 (t, *J* = 7.4 Hz, 1H), 7.53 (t, *J* = 7.4 Hz, 2H), 6.84–6.81 (m, 2H), 6.56 (d, *J* = 4.0 Hz, 1H), 6.15–6.11 (m, 2H), 5.02 (s, 2H), 3.88–3.67 (m, 4H), 3.67–3.61 (m, 1H), 2.04 (s, 3H), 2.01–1.86 (m, 5H), 0.95 (dd, *J* = 3.6 Hz, *J* = 6.6 Hz, 6H), 0.76 (t, *J* = 7.0 Hz, 3H), 0.54 (t, *J* = 7.0 Hz, 6H). ¹³C NMR (75 MHz, CDCl₃) δ (ppm) 163.45, 159.51, 153.35, 143.54, 140.83, 137.10, 134.27, 129.98, 129.17, 129.06, 126.82, 125.42, 112.04, 111.26, 108.14, 83.02, 64.74, 57.11, 46.43, 40.72, 29.31, 28.43, 19.68, 18.80, 16.35, 16.04, 8.13. ESI-HRMS calcd for C₃₁H₄₂N₂O₅S [M+Na]⁺ 577.2814, found 577.2720.

4.3.7. *(R)*-1-ethyl-*N*-(1-hydroxy-3-methylbutan-2-yl)-5-(3-(3-methyl-4-((phenylsulfonyl)methoxy)phenyl)pentan-3-yl)-1H-pyrrole-2-carboxamide (**15g**)

Petroleum ether/ethyl acetate (4/1). oil. 73% yield. ¹H NMR (300 MHz, CDCl₃) δ (ppm) 7.97 (d, *J* = 7.2 Hz, 2H), 7.66 (t, *J* = 7.4 Hz, 1H), 7.55 (t, *J* = 7.4 Hz, 2H), 6.85–6.81 (m, 2H), 6.68 (d, *J* = 8.5 Hz, 1H), 6.56 (d, *J* = 4.0 Hz, 1H), 6.13 (d, *J* = 4.0 Hz, 1H), 5.03 (s, 2H), 3.89–3.63 (m, 5H), 2.04 (s, 3H), 2.00–1.87 (m, 5H), 0.95 (dd, *J* = 3.6 Hz, *J* = 6.6 Hz, 6H), 0.78 (t, *J* = 6.9 Hz, 3H), 0.55 (t, *J* = 7.0 Hz, 6H). ¹³C NMR (75 MHz, CDCl₃) δ (ppm) 163.42, 159.46, 153.35, 143.50, 140.83, 137.09, 134.28, 129.98, 129.16, 129.05, 126.81, 125.42, 112.03, 111.26, 108.13, 83.00, 64.65, 57.05, 46.42, 40.70, 29.66, 29.29, 28.42, 26.89, 19.67, 18.79, 16.34, 16.03, 8.12. ESI-HRMS calcd for C₃₁H₄₂N₂O₅S [M+Na]⁺ 577.2814, found 577.2718.

4.3.8. *1-ethyl-N-(3-hydroxypropyl)-5-(3-(3-methyl-4-((phenylsulfonyl)methoxy)phenyl)pentan-3-yl)-1H-pyrrole-2-carboxamide (15h)*

Petroleum ether/ethyl acetate (3/1). oil. 76% yield. ¹H NMR (300 MHz, CDCl₃) δ (ppm) 7.97 (d, *J* = 7.4 Hz, 2H), 7.67 (t, *J* = 7.4 Hz, 1H), 7.56 (t, *J* = 7.7 Hz, 2H), 6.85–6.80 (m, 2H), 6.68 (d, *J* = 8.6 Hz, 1H), 6.53 (d, *J* = 4.0 Hz, 1H), 6.13 (d, *J* = 4.0 Hz, 1H), 5.03 (s, 2H), 3.81 (q, *J* = 6.9 Hz, 2H), 3.63 (t, *J* = 5.5 Hz, 2H), 3.49 (q, *J* = 5.5 Hz, 2H), 2.05 (s, 3H), 2.03–1.90 (m, 4H), 1.74–1.66 (m, 2H), 0.78 (t, *J* = 6.9 Hz, 3H), 0.56 (t, *J* = 7.3 Hz, 6H). ¹³C NMR (75 MHz, CDCl₃) δ (ppm) 163.42, 153.31, 143.46, 140.80, 134.25, 129.93, 129.13, 129.01, 126.77, 125.37, 125.05, 112.00, 111.33, 108.18, 82.97, 59.10, 46.39, 40.70, 36.39, 35.72, 32.65, 29.61, 28.37, 16.30, 16.01, 8.09, 0.94. ESI-HRMS calcd for C₂₉H₃₈N₂O₅S [M+Na]⁺ 549.2501, found 549.2405.

4.3.9. *(S)-N-(1,4-dihydroxybutan-2-yl)-1-ethyl-5-(3-(3-methyl-4-((phenylsulfonyl)methoxy)phenyl)pentan-3-yl)-1H-pyrrole-2-carboxamide (15i)*

Petroleum ether/ethyl acetate (5/1). oil. 81% yield. ¹H NMR (300 MHz, CDCl₃) δ (ppm) 7.96 (d, *J* = 7.4 Hz, 2H), 7.65 (t, *J* = 7.4 Hz, 1H), 7.55 (t, *J* = 7.7 Hz, 2H), 6.83–6.81 (m, 2H), 6.65 (d, *J* = 8.6 Hz, 1H), 6.62 (d, *J* = 4.0 Hz, 1H), 6.13 (d, *J* = 4.0 Hz, 1H), 5.03 (s, 2H), 4.20–4.13 (m, 1H), 3.92–3.80 (m, 1H), 3.77–3.58 (m, 5H), 2.05 (s, 3H), 2.01–1.86 (m, 4H), 1.86–1.78 (m, 1H), 1.71–1.63 (m, 1H), 0.78 (t, *J* = 6.9 Hz, 3H), 0.58–0.52 (m, 6H). ¹³C NMR (75 MHz, CDCl₃) δ (ppm) 163.36, 162.60, 153.31, 143.72, 140.76, 137.00, 134.28, 129.91, 129.15, 129.00, 126.77, 125.38, 124.82, 112.03, 111.99, 108.30, 82.96, 65.37, 58.79, 48.43, 46.40, 40.72, 36.48, 34.47, 29.61, 28.43, 16.30, 16.01, 8.11, 8.06, 0.94. ESI-HRMS calcd for C₃₀H₄₀N₂O₆S [M+Na]⁺ 579.2607, found 579.2510.

4.3.10. *(R)-N-(1,4-dihydroxybutan-2-yl)-1-ethyl-5-(3-(3-methyl-4-((phenylsulfonyl)methoxy)phenyl)pentan-3-yl)-1H-pyrrole-2-carboxamide (15j)*

Petroleum ether/ethyl acetate (3/1). oil. 69% yield. ¹H NMR (300 MHz, CDCl₃) δ (ppm) 7.97 (d, *J* = 7.3 Hz, 2H), 7.68 (t, *J* = 7.4 Hz, 1H), 7.56 (t, *J* = 7.4 Hz, 2H), 6.86–6.81 (m, 2H), 6.70–6.63 (m, 2H), 6.15 (d, *J* = 4.0 Hz, 1H), 5.04 (s, 2H), 4.24–4.18 (m, 1H), 3.87–3.70 (m, 6H), 2.90–2.81 (m, 2H), 2.06 (s, 3H), 1.99–1.90 (m, 4H), 0.80 (t, *J* = 6.9 Hz, 3H), 0.57–0.56 (m, 6H). ¹³C NMR (75 MHz, CDCl₃) δ (ppm) 163.40, 153.36, 143.86, 140.79, 137.07, 134.30, 129.96, 129.18, 129.05, 126.83, 125.42, 124.80, 112.06, 111.99, 108.37, 83.02, 65.63, 58.91, 48.45, 46.45, 40.79, 34.51, 28.45, 16.35, 16.06, 8.15, 8.10. ESI-HRMS calcd for C₃₀H₄₀N₂O₆S [M+Na]⁺ 579.2607, found 579.2515.

4.3.11. *(S)-N-(1,5-dihydroxypentan-2-yl)-1-ethyl-5-(3-(3-methyl-4-((phenylsulfonyl)methoxy)phenyl)pentan-3-yl)-1H-pyrrole-2-carboxamide (15k)*

Petroleum ether/ethyl acetate (3/1). oil. 71% yield. ¹H NMR (300 MHz, CDCl₃) δ (ppm) 7.97 (d, *J* = 7.3 Hz, 2H), 7.67 (tt, *J* = 7.4 Hz, *J* = 1.3 Hz, 1H), 7.56 (t, *J* = 7.4 Hz, 2H), 6.85–6.82 (m, 2H), 6.68 (d, *J* = 8.4 Hz, 1H), 6.60 (d, *J* = 4.0 Hz, 1H), 6.13 (d, *J* = 4.0 Hz, 1H), 5.03 (s, 2H), 4.05–4.01 (m, 1H), 3.87–3.74 (m, 2H), 3.72–3.57 (m, 4H), 2.06 (s, 3H), 2.01–1.91 (m, 4H), 1.73–1.59 (m, 4H), 0.79 (t, *J* = 6.8 Hz, 3H), 0.56 (t, *J* = 7.0 Hz, 6H). ¹³C NMR (75 MHz, CDCl₃) δ (ppm) 172.64, 163.23, 153.35, 143.59, 140.84, 137.07, 134.29, 129.97, 129.18, 129.05, 126.81, 125.42, 125.21, 119.55, 112.06, 111.65, 108.24, 83.02, 65.93, 62.36, 51.41, 46.44, 40.76, 29.66, 28.68, 28.43, 27.90, 16.35, 16.07, 8.13. ESI-HRMS calcd for C₃₁H₄₂N₂O₆S [M+Na]⁺ 593.2764, found 593.2677.

4.3.12. *(R)-N-(1,5-dihydroxypentan-2-yl)-1-ethyl-5-(3-(3-methyl-4-((phenylsulfonyl)methoxy)phenyl)pentan-3-yl)-1H-pyrrole-2-carboxamide (15l)*

Petroleum ether/ethyl acetate (4/1). oil. 80% yield. ¹H NMR (300 MHz, CDCl₃) δ (ppm) 7.97 (d, *J* = 7.3 Hz, 2H), 7.67 (tt, *J* = 7.4 Hz, *J* = 1.3 Hz, 1H), 7.55 (t, *J* = 7.4 Hz, 2H), 6.84–6.81 (m, 2H), 6.68 (d, *J* = 8.7 Hz, 1H), 6.59 (d, *J* = 4.0 Hz, 1H), 6.13 (d, *J* = 4.0 Hz, 1H), 5.03 (s, 2H), 4.05–4.01 (m, 1H), 3.86–3.74 (m, 2H), 3.69–3.59 (m, 4H), 2.05 (s, 3H), 2.00–1.90 (m, 4H), 1.70–1.63 (m, 4H), 0.78 (t, *J* = 6.8 Hz, 3H), 0.55 (t, *J* = 7.0 Hz, 6H). ¹³C NMR (75 MHz, CDCl₃) δ (ppm) 163.21, 153.35, 143.57, 140.84, 137.07, 134.30, 129.97, 129.18, 129.05, 126.80, 125.43, 125.22, 112.07, 111.67, 108.25, 83.02, 65.86, 62.33, 51.38, 46.43, 40.76, 29.65, 28.68, 28.43, 27.89, 16.35, 16.07, 8.13. ESI-HRMS calcd for C₃₁H₄₂N₂O₆S [M+Na]⁺ 593.2764, found 593.2671.

4.4. General procedure 3 - synthesis of compounds 16a-k

To a stirred solution of appropriate ester **14a–14k** (0.33 mmol) in a mixture of MeOH/H₂O 10:1 (40 mL) was added KOH (185.1 mg, 3.30 mmol) at 70 °C. After 24 h, the solution was evaporated, water (20 mL) and EtOAc (80 mL) was added. The organic phase were washed with brine and dried over anhydrous Na₂SO₄, filtered and concentrated. The residue was purified by silica gel column chromatography eluting with appropriate mixture as indicated in each case.

4.4.1. *(1-ethyl-5-(3-(3-methyl-4-((phenylsulfonyl)methoxy)phenyl)pentan-3-yl)-1H-pyrrole-2-carbonyl)-L-alanine (16a)*

Dichloromethane/methanol (50/1). oil. 66% yield. ¹H NMR (300 MHz, CDCl₃) δ (ppm) 7.97 (d, *J* = 7.2 Hz, 2H), 7.66 (t, *J* = 7.3 Hz, 1H), 7.55 (t, *J* = 7.3 Hz, 2H), 6.85–6.80 (m, 2H), 6.63 (d, *J* = 4.0 Hz, 1H), 6.30 (d, *J* = 6.6 Hz, 1H), 6.16 (d, *J* = 4.0 Hz, 1H), 5.04 (s, 2H), 4.62–4.55 (m, 1H), 3.87–3.70 (m, 2H), 2.06 (s, 3H), 2.01–1.92 (m, 4H), 1.50 (d, *J* = 7.1 Hz, 3H), 0.79 (t, *J* = 6.9 Hz, 3H), 0.57 (t, *J* = 7.3 Hz, 6H). ¹³C NMR (75 MHz, CDCl₃) δ (ppm) 175.52, 162.12, 152.92, 143.91, 140.22, 133.84, 129.50, 128.71, 128.60, 126.41, 124.93, 123.77, 112.12, 111.59, 108.14, 82.53, 47.92, 46.03, 40.43, 27.96, 17.26, 15.89, 15.52, 7.65. ESI-HRMS calcd for C₂₉H₃₆N₂O₆S [M+Na]⁺ 563.2294, found 563.2202.

4.4.2. *(1-ethyl-5-(3-(3-methyl-4-((phenylsulfonyl)methoxy)phenyl)pentan-3-yl)-1H-pyrrole-2-carbonyl)glycine (16b)*

Dichloromethane/methanol (50/1). oil. 73% yield. ¹H NMR (300 MHz, CDCl₃) δ (ppm) 7.98 (d, *J* = 7.3 Hz, 2H), 7.67 (tt, *J* = 7.4 Hz, *J* = 1.3 Hz, 1H), 7.56 (t, *J* = 7.4 Hz, 2H), 6.85–6.81 (m, 2H), 6.65 (d, *J* = 4.0 Hz, 1H), 6.36 (t, *J* = 5.2 Hz, 1H), 6.18 (d, *J* = 4.0 Hz, 1H), 5.04 (s, 2H), 4.14 (d, *J* = 5.1 Hz, 2H), 3.79 (q, *J* = 7.0 Hz, 2H), 2.06 (s, 3H), 2.02–1.92 (m, 4H), 0.80 (t, *J* = 7.0 Hz, 3H), 0.57 (t, *J* = 7.3 Hz, 6H). ¹³C NMR (75 MHz, DMSO) δ (ppm) 172.87, 162.27, 152.91, 143.81, 140.24, 133.83, 129.51, 128.71, 128.59, 126.40, 124.93, 123.76, 112.12, 111.58, 108.15, 82.53, 46.01, 41.12, 40.43, 27.95, 15.88, 15.52, 7.65. ESI-HRMS calcd for C₂₈H₃₄N₂O₆S [M+Na]⁺ 549.2138, found 549.2078.

4.4.3. *(1-ethyl-5-(3-(3-methyl-4-((phenylsulfonyl)methoxy)phenyl)pentan-3-yl)-1H-pyrrole-2-carbonyl)-D-alanine (16c)*

Dichloromethane/methanol (100/1). oil. 63% yield. ¹H NMR (300 MHz, CDCl₃) δ (ppm) 7.97 (d, *J* = 7.2 Hz, 2H), 7.67 (t, *J* = 7.3 Hz, 1H), 7.55 (t, *J* = 7.3 Hz, 2H), 6.84–6.80 (m, 2H), 6.68 (d, *J* = 8.5 Hz, 1H), 6.64 (d, *J* = 4.0 Hz, 1H), 6.16 (d, *J* = 4.0 Hz, 1H), 5.04 (s, 2H), 4.64–4.55 (m, 1H), 3.87–3.67 (m, 2H), 2.05 (s, 3H), 2.04–1.91 (m, 4H), 1.49 (d, *J* = 7.1 Hz, 3H), 0.78 (t, *J* = 6.9 Hz, 3H), 0.56 (t, *J* = 7.3 Hz, 6H). ¹³C NMR (75 MHz, CDCl₃) δ (ppm) 176.35, 162.40, 153.34, 144.20, 140.67, 137.02, 134.27, 129.94, 129.15, 129.02, 126.82, 125.37, 124.32, 112.50, 112.03, 108.52, 82.96, 48.25, 46.44, 40.84, 29.62, 28.39, 17.84, 16.31, 15.95, 8.08, 0.95. ESI-HRMS calcd for

$C_{29}H_{36}N_2O_6S$ [$M+Na$] $^+$ 563.2294, found 563.2186.

4.4.4. *1-(1-ethyl-5-(3-(3-methyl-4-((phenylsulfonyl)methoxy)phenyl)pentan-3-yl)-1H-pyrrole-2-carboxamido)cyclopropane-1-carboxylic acid (16d)*

Dichloromethane/methanol (80/1). oil. 72% yield. 1H NMR (300 MHz, $CDCl_3$) δ (ppm) 7.96 (d, $J = 7.4$ Hz, 2H), 7.65 (t, $J = 7.4$ Hz, 1H), 7.54 (t, $J = 7.7$ Hz, 2H), 6.82–6.79 (m, 2H), 6.66 (d, $J = 8.6$ Hz, 1H), 6.57 (d, $J = 4.0$ Hz, 1H), 6.12 (d, $J = 4.0$ Hz, 1H), 5.03 (s, 2H), 3.77 (q, $J = 6.9$ Hz, 2H), 2.04 (s, 3H), 2.02–1.89 (m, 4H), 1.63–1.58 (m, 2H), 1.20–1.18 (m, 2H), 0.78 (t, $J = 6.9$ Hz, 3H), 0.54 (t, $J = 7.3$ Hz, 6H). ^{13}C NMR (75 MHz, $CDCl_3$) δ (ppm) 177.23, 163.47, 153.29, 144.04, 140.69, 137.00, 134.28, 129.92, 129.15, 129.00, 126.76, 125.38, 124.54, 112.35, 112.00, 108.36, 82.96, 46.40, 40.85, 36.63, 33.36, 29.62, 28.37, 18.00, 16.32, 15.93, 8.08. ESI-HRMS calcd for $C_{30}H_{36}N_2O_6S$ [$M+Na$] $^+$ 575.2294, found 575.2197.

4.4.5. *(1-ethyl-5-(3-(3-methyl-4-((phenylsulfonyl)methoxy)phenyl)pentan-3-yl)-1H-pyrrole-2-carbonyl)-L-valine (16e)*

Dichloromethane/methanol (80/1). oil. 68% yield. 1H NMR (300 MHz, $CDCl_3$) δ (ppm) 7.97 (d, $J = 7.2$ Hz, 2H), 7.66 (t, $J = 7.3$ Hz, 1H), 7.54 (t, $J = 7.3$ Hz, 2H), 6.85–6.81 (m, 2H), 6.69–6.64 (m, 2H), 6.16 (d, $J = 4.0$ Hz, 1H), 5.04 (s, 2H), 4.60–4.56 (m, 1H), 3.85–3.71 (m, 2H), 2.30–2.24 (m, 1H), 2.05 (s, 3H), 2.01–1.93 (m, 4H), 0.98 (t, $J = 7.9$ Hz, 6H), 0.76 (t, $J = 7.0$ Hz, 3H), 0.58–0.54 (m, 6H). ^{13}C NMR (75 MHz, $CDCl_3$) δ (ppm) 175.97, 162.43, 153.36, 144.03, 140.74, 137.08, 134.28, 129.98, 129.17, 129.06, 126.84, 125.42, 124.77, 112.12, 112.05, 108.39, 83.01, 57.14, 46.45, 40.80, 30.89, 28.42, 19.17, 17.85, 16.34, 15.99, 8.13, 8.11. ESI-HRMS calcd for $C_{29}H_{36}N_2O_6S$ [$M+Na$] $^+$ 591.2607, found 591.2511.

4.4.6. *(1-ethyl-5-(3-(3-methyl-4-((phenylsulfonyl)methoxy)phenyl)pentan-3-yl)-1H-pyrrole-2-carbonyl)-D-valine (16f)*

Dichloromethane/methanol (80/1). oil. 65% yield. 1H NMR (300 MHz, $CDCl_3$) δ (ppm) 7.98 (d, $J = 7.2$ Hz, 2H), 7.67 (t, $J = 7.5$ Hz, 1H), 7.56 (t, $J = 7.5$ Hz, 2H), 6.86–6.82 (m, 2H), 6.68 (d, $J = 8.5$ Hz, 1H), 6.64 (d, $J = 4.0$ Hz, 1H), 6.17 (d, $J = 4.0$ Hz, 1H), 5.04 (s, 2H), 4.56 (dd, $J = 5.0$ Hz, $J = 8.3$ Hz, 1H), 3.87–3.72 (m, 2H), 2.34–2.25 (m, 1H), 2.06 (s, 3H), 2.02–1.92 (m, 4H), 1.01 (t, $J = 8.0$ Hz, 6H), 0.78 (t, $J = 6.8$ Hz, 3H), 0.59–0.55 (m, 6H). ^{13}C NMR (75 MHz, $CDCl_3$) δ (ppm) 175.83, 162.45, 153.37, 146.89, 144.05, 140.74, 137.08, 134.28, 129.98, 129.17, 129.06, 126.85, 125.42, 124.77, 112.12, 112.05, 108.39, 83.01, 57.17, 46.45, 40.80, 30.85, 29.66, 28.43, 19.18, 17.85, 16.34, 15.99, 8.13, 8.10. ESI-HRMS calcd for $C_{31}H_{40}N_2O_6S$ [$M+Na$] $^+$ 591.2607, found 591.2520.

4.4.7. *3-(1-ethyl-5-(3-(3-methyl-4-((phenylsulfonyl)methoxy)phenyl)pentan-3-yl)-1H-pyrrole-2-carboxamido)propanoic acid (16g)*

Dichloromethane/methanol (75/1). oil. 69% yield. 1H NMR (300 MHz, $CDCl_3$) δ (ppm) 7.95 (d, $J = 7.4$ Hz, 2H), 7.65 (t, $J = 7.4$ Hz, 1H), 7.54 (t, $J = 7.7$ Hz, 2H), 6.83–6.80 (m, 2H), 6.66 (d, $J = 8.6$ Hz, 1H), 6.53 (d, $J = 4.0$ Hz, 1H), 6.11 (d, $J = 4.0$ Hz, 1H), 5.03 (s, 2H), 3.78 (q, $J = 7.0$ Hz, 2H), 3.57 (q, $J = 5.8$ Hz, 2H), 2.60 (t, $J = 5.8$ Hz, 2H), 2.04 (s, 3H), 2.02–1.89 (m, 4H), 0.77 (t, $J = 6.9$ Hz, 3H), 0.54 (t, $J = 7.3$ Hz, 6H). ^{13}C NMR (75 MHz, $CDCl_3$) δ (ppm) 175.98, 163.10, 162.40, 153.27, 143.40, 140.81, 137.00, 134.27, 129.92, 129.14, 128.99, 126.73, 125.38, 125.16, 112.00, 111.62, 108.21, 82.95, 46.37, 40.74, 36.70, 34.63, 34.11, 29.60, 28.37, 16.29, 16.00, 8.09. ESI-HRMS calcd for $C_{29}H_{36}N_2O_6S$ [$M+Na$] $^+$ 563.2294, found 563.2199.

4.4.8. *(1-ethyl-5-(3-(3-methyl-4-((phenylsulfonyl)methoxy)phenyl)pentan-3-yl)-1H-pyrrole-2-carbonyl)-L-aspartic acid (16h)*

Dichloromethane/methanol (75/1). oil. 66% yield. 1H NMR (300 MHz, $CDCl_3$) δ (ppm) 7.96 (d, $J = 7.4$ Hz, 2H), 7.65 (t, $J = 7.4$ Hz,

1H), 7.55 (t, $J = 7.7$ Hz, 2H), 6.97 (d, $J = 8.6$ Hz, 1H), 6.84–6.81 (m, 2H), 6.66 (d, $J = 4.0$ Hz, 1H), 6.16 (d, $J = 4.0$ Hz, 1H), 5.04 (s, 2H), 4.96–4.90 (m, 1H), 3.85–3.68 (m, 2H), 3.16–3.08 (m, 1H), 2.95–2.94 (m, 1H), 2.06 (s, 3H), 2.01–1.91 (m, 4H), 0.79 (t, $J = 6.9$ Hz, 3H), 0.56 (t, $J = 7.3$ Hz, 6H). ^{13}C NMR (75 MHz, $CDCl_3$) δ (ppm) 175.10, 174.37, 163.10, 162.22, 153.33, 144.34, 140.68, 134.27, 129.93, 129.15, 129.02, 126.81, 125.40, 124.17, 112.99, 112.04, 108.64, 82.96, 48.43, 46.45, 40.88, 36.70, 36.06, 28.39, 16.31, 15.97, 8.09, 0.95. ESI-HRMS calcd for $C_{30}H_{36}N_2O_8S$ [$M+Na$] $^+$ 607.2192, found 607.2104.

4.4.9. *(1-ethyl-5-(3-(3-methyl-4-((phenylsulfonyl)methoxy)phenyl)pentan-3-yl)-1H-pyrrole-2-carbonyl)-D-aspartic acid (16i)*

Dichloromethane/methanol (50/1). oil. 73% yield. 1H NMR (300 MHz, $CDCl_3$) δ (ppm) 7.96 (d, $J = 7.3$ Hz, 2H), 7.65 (t, $J = 7.4$ Hz, 1H), 7.54 (t, $J = 7.4$ Hz, 2H), 6.86–6.81 (m, 2H), 6.70–6.63 (m, 2H), 6.15 (d, $J = 4.0$ Hz, 1H), 5.04 (s, 2H), 4.96–4.91 (m, 1H), 3.80–3.73 (m, 2H), 2.04 (s, 3H), 1.99–1.90 (m, 4H), 0.77 (t, $J = 6.9$ Hz, 3H), 0.57–0.56 (m, 6H). ^{13}C NMR (75 MHz, $CDCl_3$) δ (ppm) 175.81, 162.25, 153.37, 144.51, 140.65, 137.05, 134.30, 129.87, 129.18, 129.04, 126.81, 125.48, 124.05, 113.27, 112.14, 108.78, 82.97, 48.65, 46.49, 40.92, 36.40, 29.66, 28.44, 16.34, 16.01, 8.13. ESI-HRMS calcd for $C_{30}H_{36}N_2O_8S$ [$M+H$] $^+$ 585.2192, found 585.2282.

4.4.10. *(1-ethyl-5-(3-(3-methyl-4-((phenylsulfonyl)methoxy)phenyl)pentan-3-yl)-1H-pyrrole-2-carbonyl)-L-glutamic acid (16j)*

Dichloromethane/methanol (50/1). oil. 55% yield. 1H NMR (300 MHz, $CDCl_3$) δ (ppm) 7.96 (d, $J = 7.4$ Hz, 2H), 7.65 (t, $J = 7.5$ Hz, 1H), 7.54 (t, $J = 7.5$ Hz, 2H), 6.82–6.79 (m, 2H), 6.69–6.66 (m, 2H), 6.16 (d, $J = 4.0$ Hz, 1H), 5.04 (s, 2H), 4.67–4.65 (m, 1H), 3.83–3.68 (m, 2H), 2.54–2.48 (m, 2H), 2.30–2.11 (m, 2H), 2.05 (s, 3H), 2.00–1.94 (m, 4H), 0.76 (t, $J = 6.5$ Hz, 3H), 0.55 (t, $J = 7.0$ Hz, 6H). ^{13}C NMR (75 MHz, $CDCl_3$) δ (ppm) 177.95, 176.05, 162.35, 153.39, 144.48, 140.68, 137.07, 134.29, 129.94, 129.17, 129.05, 126.87, 125.42, 124.12, 112.83, 112.12, 108.70, 83.02, 51.64, 46.50, 40.92, 29.76, 28.43, 26.66, 16.33, 15.98, 8.11. ESI-HRMS calcd for $C_{31}H_{38}N_2O_8S$ [$M+Na$] $^+$ 621.2349, found 621.2261.

4.4.11. *(1-ethyl-5-(3-(3-methyl-4-((phenylsulfonyl)methoxy)phenyl)pentan-3-yl)-1H-pyrrole-2-carbonyl)-D-glutamic acid (16k)*

Dichloromethane/methanol (50/1). oil. 62% yield. 1H NMR (300 MHz, $CDCl_3$) δ (ppm) 7.97 (d, $J = 7.4$ Hz, 2H), 7.66 (t, $J = 7.5$ Hz, 1H), 7.55 (t, $J = 7.5$ Hz, 2H), 6.83–6.80 (m, 2H), 6.69–6.66 (m, 2H), 6.16 (d, $J = 4.0$ Hz, 1H), 5.04 (s, 2H), 4.67 (q, $J = 6.5$ Hz, 1H), 3.84–3.69 (m, 2H), 2.54–2.51 (m, 2H), 2.29–2.16 (m, 2H), 2.05 (s, 3H), 2.01–1.87 (m, 4H), 0.77 (t, $J = 6.5$ Hz, 3H), 0.56 (t, $J = 7.0$ Hz, 6H). ^{13}C NMR (75 MHz, $CDCl_3$) δ (ppm) 177.67, 175.66, 162.52, 153.35, 144.44, 140.67, 136.99, 134.33, 129.90, 129.20, 129.03, 126.81, 125.46, 124.12, 113.02, 112.13, 108.70, 82.98, 51.68, 46.48, 40.89, 30.03, 29.66, 28.42, 26.84, 16.33, 15.99, 8.13. ESI-HRMS calcd for $C_{31}H_{38}N_2O_8S$ [$M+Na$] $^+$ 621.2349, found 621.2262.

4.5. General procedure 4 - synthesis of compounds **19a-b**

To a solution of compound **18** (0.35 g, 0.85 mmol) in DMF (50 mL), NaH (30.46 mg, 1.27 mmol) was added portionwise at 0 °C. After stirring for 0.5 h, appropriate chloromethyl substituted sulfide (1.23 mmol) was added. The reaction mixture was stirred at 70 °C for 12 h and then H₂O (100 mL) was added dropwise followed by EtOAc (80 mL). Organic phase was separated and washed with brine and dried over anhydrous Na₂SO₄, filtered and concentrated. The residue was purified by silica gel column chromatography eluting with appropriate mixture as indicated in each case.

4.5.1. *N*-(2-(diethylamino)ethyl)-1-ethyl-5-(3-(3-methyl-4-((methylthio)methoxy)phenyl)pentan-3-yl)-1*H*-pyrrole-2-carboxamide (**19a**)

Dichloromethane/methanol (100/1). oil. 61% yield. ¹H NMR (300 MHz, CDCl₃) δ (ppm) 6.90–6.86 (m, 2H), 6.77 (s, 1H), 6.60 (d, *J* = 2.5 Hz, 1H), 6.15 (d, *J* = 2.5 Hz, 1H), 5.11 (s, 2H), 3.88 (q, *J* = 6.6 Hz, 2H), 3.42 (q, *J* = 5.5 Hz, 2H), 2.68–2.59 (m, 6H), 2.23 (s, 3H), 2.17 (s, 3H), 2.09–1.97 (m, 4H), 1.08 (t, *J* = 7.0 Hz, 6H) 0.83 (t, *J* = 6.6 Hz, 3H), 0.59 (t, *J* = 7.3 Hz, 6H). ¹³C NMR (75 MHz, CDCl₃) δ (ppm) 162.39, 143.40, 139.44, 129.77, 127.21, 125.18, 112.60, 111.31, 108.08, 72.74, 51.91, 47.04, 46.38, 40.83, 36.44, 28.44, 16.54, 16.11, 14.75, 11.54, 8.23. ESI-HRMS calcd for C₂₇H₄₃N₃O₂S [M+H]⁺ 474.3076, found 474.3166.

4.5.2. *N*-(2-(diethylamino)ethyl)-1-ethyl-5-(3-(3-methyl-4-((phenylthio)methoxy)phenyl)pentan-3-yl)-1*H*-pyrrole-2-carboxamide (**19b**)

Dichloromethane/methanol (100/1). oil. 51% yield. ¹H NMR (300 MHz, CDCl₃) δ (ppm) 7.49–7.48 (m, 1H), 7.47–7.46 (m, 1H), 7.32–7.27 (m, 2H), 7.25–7.20 (m, 1H), 6.92–6.87 (m, 2H), 6.78 (d, *J* = 8.4 Hz, 1H), 6.57 (d, *J* = 4.0 Hz, 1H), 6.167.56 (t, *J* = 7.3 Hz, 2H), 6.86–6.81 (m, 3H), 6.64 (d, *J* = 4.0 Hz, 1H), 6.16 (d, *J* = 4.0 Hz, 1H), 5.45 (s, 2H), 3.90 (q, *J* = 7.0 Hz, 2H), 3.40 (q, *J* = 5.6 Hz, 2H), 2.64–2.55 (m, 6H), 2.13 (s, 3H), 2.08–1.96 (m, 4H), 1.06 (t, *J* = 7.2 Hz, 6H), 0.84 (t, *J* = 7.0 Hz, 3H), 0.60 (t, *J* = 7.3 Hz, 6H). ¹³C NMR (75 MHz, CDCl₃) δ (ppm) 162.38, 153.04, 143.32, 139.70, 130.51, 129.86, 128.95, 127.42, 127.03, 125.72, 125.18, 112.69, 111.08, 108.01, 73.22, 51.79, 46.92, 46.39, 40.85, 36.61, 29.70, 28.45, 16.63, 16.11, 11.81, 8.23. ESI-HRMS calcd for C₃₂H₄₅N₃O₂S [M+H]⁺ 536.3232, found 536.3325.

4.6. *N*-(2-(diethylamino)ethyl)-1-ethyl-5-(3-(3-methyl-4-((methylsulfonyl)methoxy)phenyl)pentan-3-yl)-1*H*-pyrrole-2-carboxamide (**20a**)

To a stirred solution of **19a** (0.77 g, 1.63 mmol) in a mixture of EtOH/H₂O 10:1 (40 mL) was added potassium peroxydisulfate (2.74 g, 16.32 mmol). After 24 h, the solution was evaporated, water (20 mL) and EtOAc (80 mL) was added. The organic phase were washed with brine and dried over anhydrous Na₂SO₄, filtered and concentrated. The residue was purified by column chromatography with petroleum ether/ethyl acetate (10/1, v/v) to give compound **20a** as oil (0.65 g, 79% yield). ¹H NMR (300 MHz, CDCl₃) δ (ppm) 6.95–6.90 (m, 2H), 6.83 (d, *J* = 8.8 Hz, 1H), 6.63 (s, 1H), 6.16 (d, *J* = 4.1 Hz, 1H), 4.94 (s, 2H), 3.86 (q, *J* = 7.0 Hz, 2H), 3.43 (q, *J* = 5.5 Hz, 2H), 3.00 (s, 3H), 2.70–2.61 (m, 6H), 2.23 (s, 3H), 2.07–1.99 (m, 4H), 1.10 (t, *J* = 7.0 Hz, 6H) 0.84 (t, *J* = 7.0 Hz, 3H), 0.59 (t, *J* = 7.3 Hz, 6H). ¹³C NMR (75 MHz, CDCl₃) δ (ppm) 130.30, 125.81, 112.60, 111.31, 108.26, 82.49, 51.89, 47.06, 46.54, 40.86, 38.63, 36.59, 29.77, 16.53, 16.25, 11.74, 8.26. ESI-HRMS calcd for C₂₇H₄₃N₃O₄S [M+H]⁺ 506.2974, found 506.3066.

4.7. General procedure 5 - synthesis of compounds **26a-b**

To a solution of compound **25** (0.35 g, 0.85 mmol) in DMF (50 mL), NaH (30.46 mg, 1.27 mmol) was added portionwise at 0 °C. After stirring for 0.5 h, appropriate chloromethyl substituted sulfide (1.23 mmol) was added. The reaction mixture was stirred at 70 °C for 12 h and then H₂O (100 mL) was added dropwise followed by EtOAc (80 mL). Organic phase was separated and washed with brine and dried over anhydrous Na₂SO₄, filtered and concentrated. The residue was purified by silica gel column chromatography eluting with appropriate mixture as indicated in each case.

4.7.1. *N*-(2-(diethylamino)ethyl)-1-ethyl-4-(3-(3-methyl-4-((methylthio)methoxy)phenyl)pentan-3-yl)-1*H*-pyrrole-2-carboxamide (**26a**)

Dichloromethane/methanol (30/1). oil. 60% yield. ¹H NMR (300 MHz, CDCl₃) δ (ppm) 7.04–7.02 (m, 2H), 6.75 (d, *J* = 9.0 Hz, 1H), 6.48 (s, 2H), 5.12 (s, 2H), 4.30 (q, *J* = 7.0 Hz, 2H), 3.57 (q, *J* = 5.5 Hz, 2H), 2.87–2.79 (m, 6H), 2.25 (s, 3H), 2.20 (s, 3H), 1.97–1.89 (m, 4H), 1.34 (t, *J* = 7.1 Hz, 3H) 1.18 (t, *J* = 7.0 Hz, 6H), 0.65 (t, *J* = 7.3 Hz, 6H). ¹³C NMR (75 MHz, CDCl₃) δ (ppm) 162.06, 152.97, 140.98, 130.79, 130.49, 126.42, 125.76, 124.36, 124.32, 111.82, 111.33, 72.54, 51.81, 47.01, 45.01, 43.61, 36.78, 30.49, 17.28, 16.60, 14.75, 11.91, 8.61. ESI-HRMS calcd for C₂₇H₄₃N₃O₂S [M+H]⁺ 474.3076, found 474.3171.

4.7.2. *N*-(2-(diethylamino)ethyl)-1-ethyl-4-(3-(3-methyl-4-((phenylthio)methoxy)phenyl)pentan-3-yl)-1*H*-pyrrole-2-carboxamide (**26b**)

Dichloromethane/methanol (30/1). oil. 67% yield. ¹H NMR (300 MHz, CDCl₃) δ (ppm) 7.52–7.49 (m, 2H), 7.33–7.27 (m, 2H), 7.24–7.21 (m, 1H), 7.07–7.03 (m, 2H), 6.77 (d, *J* = 8.1 Hz, 1H), 6.52 (d, *J* = 1.9 Hz, 1H), 6.22 (d, *J* = 1.9 Hz, 1H), 5.46 (s, 2H), 4.32 (q, *J* = 7.1 Hz, 2H), 3.39 (q, *J* = 5.8 Hz, 2H), 2.63–2.53 (m, 6H), 2.17 (s, 3H), 1.92 (q, *J* = 7.3 Hz, 4H), 1.36 (t, *J* = 7.1 Hz, 3H) 1.01 (t, *J* = 7.0 Hz, 6H), 0.66 (t, *J* = 7.3 Hz, 6H). ¹³C NMR (125 MHz, CDCl₃) δ (ppm) 162.11, 152.75, 141.30, 130.80, 130.59, 130.44, 128.94, 126.97, 126.65, 125.80, 125.71, 124.41, 124.33, 112.04, 111.41, 73.24, 51.91, 51.85, 47.08, 45.08, 43.60, 36.79, 36.75, 30.55, 17.24, 16.65, 11.85, 11.81, 8.60, 8.54. ESI-HRMS calcd for C₃₂H₄₅N₃O₂S [M+H]⁺ 536.3232, found 536.3328.

4.8. General procedure 6 - synthesis of compounds **27a-b**

To a stirred solution of **26a** or **26b** (1.63 mmol) in a mixture of EtOH/H₂O 10:1 (40 mL) was added potassium peroxydisulfate (2.74 g, 16.32 mmol). After 24 h, the solution was evaporated, water (20 mL) and EtOAc (80 mL) was added. The organic phase were washed with brine and dried over anhydrous Na₂SO₄, filtered and concentrated. The residue was purified by silica gel column chromatography eluting with appropriate mixture as indicated in each case.

4.8.1. *N*-(2-(diethylamino)ethyl)-1-ethyl-4-(3-(3-methyl-4-((methylsulfonyl)methoxy)phenyl)pentan-3-yl)-1*H*-pyrrole-2-carboxamide (**27a**)

Dichloromethane/methanol (100/1). oil. 71% yield. ¹H NMR (300 MHz, CDCl₃) δ (ppm) 7.08–7.05 (m, 2H), 6.83 (d, *J* = 8.3 Hz, 1H), 6.50 (d, *J* = 1.9 Hz, 1H), 6.21 (d, *J* = 1.9 Hz, 1H), 4.94 (s, 2H), 4.31 (q, *J* = 7.1 Hz, 2H), 3.39 (q, *J* = 5.9 Hz, 2H), 3.00 (s, 3H), 2.62 (t, *J* = 6.1 Hz, 2H), 2.58 (q, *J* = 7.3 Hz, 4H), 2.24 (s, 3H), 2.20 (s, 3H), 1.91 (q, *J* = 7.3 Hz, 4H), 1.35 (t, *J* = 7.1 Hz, 3H) 1.02 (t, *J* = 7.1 Hz, 6H), 0.64 (t, *J* = 7.3 Hz, 6H). ¹³C NMR (75 MHz, CDCl₃) δ (ppm) 162.05, 153.17, 143.12, 130.89, 130.52, 126.33, 126.15, 124.24, 112.10, 111.31, 82.49, 51.90, 47.04, 45.11, 43.63, 38.48, 36.70, 30.40, 17.26, 16.48, 11.71, 8.54. ESI-HRMS calcd for C₂₇H₄₃N₃O₄S [M+H]⁺ 506.2974, found 506.3066.

4.8.2. *N*-(2-(diethylamino)ethyl)-1-ethyl-4-(3-(3-methyl-4-((phenylsulfonyl)methoxy)phenyl)pentan-3-yl)-1*H*-pyrrole-2-carboxamide (**27b**)

Dichloromethane/methanol (100/1). oil. 67% yield. ¹H NMR (300 MHz, CDCl₃) δ (ppm) 7.98 (d, *J* = 7.3 Hz, 2H), 7.65 (tt, *J* = 7.5 Hz, 1.1 Hz, 1H), 7.55 (t, *J* = 7.9 Hz, 2H), 6.98–6.97 (m, 2H), 6.68 (d, *J* = 9.3 Hz, 1H), 6.47 (d, *J* = 1.8 Hz, 1H), 6.21 (d, *J* = 1.8 Hz, 1H), 5.02 (s, 2H), 4.30 (q, *J* = 7.2 Hz, 2H), 3.40 (q, *J* = 5.8 Hz, 2H), 2.64 (t, *J* = 6.0 Hz, 6H), 2.59 (q, *J* = 7.1 Hz, 4H), 2.08 (s, 3H), 1.89 (q, *J* = 7.3 Hz, 4H), 1.34 (t, *J* = 7.2 Hz, 3H) 1.02 (t, *J* = 7.1 Hz, 6H), 0.62 (t, *J* = 7.3 Hz, 6H). ¹³C NMR (125 MHz, CDCl₃) δ (ppm) 162.09, 153.01, 142.63,

137.27, 134.22, 130.71, 130.60, 129.15, 129.10, 129.04, 129.00, 126.10, 126.08, 124.38, 124.28, 124.25, 111.62, 111.47, 111.38, 83.16, 52.00, 47.19, 45.07, 43.60, 36.60, 30.43, 17.22, 16.38, 11.55, 8.52. ESI-HRMS calcd for $C_{32}H_{45}N_3O_4S [M+H]^+$ 568.3131, found 568.3229.

4.9. MTT assay

The effects of the compounds on the proliferation of the human cell lines were evaluated by MTT (3-(4,5-dimethylthiazol-2-yl)-2,5-diphenyl-2H-tetrazolium bromide; Sigma) assay. Briefly, cells were seeded into 96-well plates for 24 h and then treated with vehicle, the desired compounds alone, or 1,25(OH) $_2$ D $_3$ as a positive control for 24 h supplemented with 10% fetal bovine serum. After incubation with 10 μ L of MTT (5 mg/mL) for 4 h, absorbance of the soluble MTT product was measured at 570 nm. The antiproliferation assay was performed in triplicate.

4.10. Small interfering RNA (siRNA) transfection

A VDR-directed siRNA and a scrambled siRNA were purchased from RIBOBIO Biotechnologies (Guangzhou, China). Transfection was carried out at a concentration of 50 nM using Lipofectamine[®]2000 Reagent (Invitrogen). Transfected cells were cultured 24 h prior to terminal assays.

4.11. BrdU ELISA assay

The effects of the representative compounds on the proliferation of the MCF-7 cells were re-evaluated by BrdU (5-Bromo-2-deoxyUridine; Abcam) assay. Briefly, negative control (siNC) or VDR-specific (siVDR) siRNA-transfected MCF-7 cells were seeded into 96-well plates for 24 h, and cultured with DMEM media supplemented 0.4% fetal bovine serum for 3 days. Then treated with vehicle, the representative compounds, or sw-22 and 1,25(OH) $_2$ D $_3$ as positive control, and incubate with BrdU for 16 h. Afterwards, BrdU incorporation was determined via a commercial available ELISA kit (Abcam). BrdU ELISA optic density (OD) at 450 nm was recorded.

4.12. VDR binding assay

The VDR binding affinity of non-secosteroidal VDR modulators were measured by PolarScreen VDR Competitor Assay following the procedure previously described [31,32]. All compounds were tested for their binding affinity at 1 μ M in triplicates. Fluorescence polarization was measured on an Ultra384 microplate reader (Biotek) using a 535 nm excitation filter (25 nm bandwidth) and 590 nm emission filter (20 nm bandwidth).

4.13. Transcription assay

Luciferase activity assay was performed using the Dual-Luciferase Reporter Assay System (Promega, Madison, WI) according to the manufacturer's instructions. HEK293 cells of 85%–90% confluence were seeded in 48-well plates. Transfections of 140 ng of TK-Spp \times 3-LUC reporter plasmid, 20 ng of pRL-TK, 30 ng of pENTER-CMV-hRXR α and 100 ng of pENTER-CMV-hVDR for each well using Lipofectamine[®]2000 Reagent (Invitrogen). Eight hours after transfection, test compounds were added. Luciferase activity assay was performed 24 h later using the Dual-Luciferase Assay System. Firefly luciferase activity was normalized to the corresponding Renilla luciferase activity. All the experiments were performed three times.

4.14. Cell cycle assay and cell apoptosis

MCF-7 cells were seeded into 6-well plate, testing compounds (1 μ M) containing 2% FBS were added, and treated for 24 h. For the cell cycle assay, cells were washed twice with ice-cold PBS, and treated with ice-cold 70% ethanol while vortexing fixed overnight at 4 °C. After centrifuging for 5 min at 1000 g, cells were washed with 1 mL ice-cold PBS, and stained with 0.5 mL mixture solution containing 465 μ L 1 \times PBS, 25 μ L propidium iodide (PI), and 10 μ L RNaseA at 37 °C for 30 min. Data were collected using Attune NxT Acoustic Focusing Cytometer (Life Technologies, Carlsbad, CA, USA) and analyzed using the ModFit LT software (Verity Software House, Inc). For analysis of cell apoptosis, the cells were collected and suspended in 0.5 mL of 1 \times binding buffer, followed by two washes with ice-cold PBS. The Annexin V-FITC Apoptosis Detection Kit (Vazyme, Nanjing, China) according to the manufacturer's protocol was used for apoptosis assay. The stained cells were analyzed by a BD Accuri[™] C6 Plus flow cytometer equipped with BD Accuri C6 Software (Becton Dickinson, San Jose, CA).

4.15. Western blot

Proteins were purified from MCF-7 cells. Proteins were separated using 10% SDS-polyacrylamide gel electrophoresis and were electrophoretically transferred to polyvinylidene fluoride (PVDF) membranes using standard procedures. The following primary antibodies were employed: Rabbit anti-p21, rabbit anti-p27, rabbit anti-Bax, and mouse anti- β -actin (Santa Cruz Biotechnology). Horseradish peroxidase-conjugated goat anti-rabbit/mouse IgG (Boster, Wuhan, China) was used as a secondary antibody. Immunoreactive protein bands were detected using an Odyssey Scanning System (LI-COR).

4.16. Microsomal stability and solubility

For the stability studies, test compounds are incubated with rat liver microsomes (Research Institute for Liver Diseases (Shanghai) Co. Ltd) in the presence of NADPH (Sigma, N5755). Compound concentrations are then measured via analytical methods, such as HPLC, at various time points, such as 0, 5, 10, 20, 30, 45, 60 and 90 min. The half-life of the test compounds is then calculated. Solubility assay done at pH 7.4 [19]. The assay measures solubility of test compound using an HPLC method to quantify the samples.

4.17. Pharmacokinetics study

Compounds **19a**, **27b** and **sw-22** were dissolved in ethanol/EL/saline (1:1:18). Male Sprague-Dawley (SD) rats ($n = 3$) weighing 180–220 g were injected with these compounds intravenously (5 mg/kg) or intraperitoneally (20 mg/kg). Blood plasma samples were collected at 0 h, 0.083 h, 0.167 h, 0.25 h, 0.5 h, 1 h, 2 h, 4 h, 8 h, 12 h, 24 h after administration of compounds, and then immediately centrifuged (12000 rpm, 10 min) to obtain plasma samples. The concentration of compounds in plasma was measure by HPLC. The pharmacokinetic parameters were calculated using Kinetica 4.4 software.

4.18. In vivo antitumor activity assay

Male athymic (BALB/c-nu) mice (10 weeks old) were obtained from the Beijing Vital River Laboratory Animal Technology Co. Ltd (Beijing, China). Our experimental protocol was reviewed and approved by the Institutional Animal Care Committee of China Pharmaceutical University. MCF-7 cells (1×10^7 cells used for each injection) were injected in the left fourth mammary fat pad of nude

mice. When the tumor volume reached approximately 50 mm³ (7 days after injecting), the mice were sorted into six groups: (1) control; (2) vehicle; (3) **19a**; (4) **27b**; (5) **sw-22**; (6) 1,25(OH)₂D₃ (n = 5), and administration was started. Compounds **19a**, **27b** and **sw-22** was injected via intraperitoneally at doses of 10 mg/kg. 1,25(OH)₂D₃ was injected via intraperitoneally at doses of 0.5 µg/kg. Compounds were prepared in ethanol/EL/saline = 1:1:18 and injected three times a week for three weeks. Tumor dimensions were determined using calipers, and the tumor volume (mm³) was calculated using the following formula: volume = length × (width)² × 0.5. The total calcium ion concentration was colorimetric determined by Methyl Timolol Blue (MTB) method in venous blood using a calcium assay kit (Nanjing Jiancheng Bioengineering institute, China).

4.19. Immunocytochemistry

Tumor tissues were fixed in 4% (w/v) neutral phosphate-buffered paraformaldehyde for 24 h, dehydrated, transparentized and embedded in paraffin. Tumor tissues were cut into 5-µm sections. The slides were gotten rid of paraffin, subjected to antigen retrieval, and quenching of endogenous peroxidase activity using 3% (v/v) H₂O₂ for 10 min. The rabbit anti-p21, rabbit anti-p27, and rabbit anti-Bax (Santa Cruz Biotechnology) were employed. Immune complexes were visualized using suitable peroxidase-coupled secondary antibodies, according to the manufacturer's protocol of PV-9000 2-step plus poly-HRP anti-mouse/rabbit IgG detection system (ZSCG-BIO, Beijing, China).

4.20. Statistical analysis

Data were expressed as means ± standard deviation from at least three independent experiments. The differences between groups were analyzed for significance (*P* < 0.05) by *t*-test when only two groups were compared or by one-way analysis of variance (ANOVA). All statistical analysis was performed using SPSS for windows version 11.0 (SPSS, Chicago, IL).

Acknowledgments

This work was supported by the National Natural Science Foundation of China (81773664, 81473153, 81703585), National Basic Research Program of China (2015CB755500), Fundamental Research Funds for the Central Universities of China (2632017PY10), and 111 Project from the Ministry of Education of China and the State Administration of Foreign Expert Affairs of China (No. 111-2-07).

Appendix A. Supplementary data

Supplementary data related to this article can be found at <https://doi.org/10.1016/j.ejmech.2018.08.085>.

References

- [1] R. Bouillon, in: *Vitamin D - Proceedings of the 12th Workshop on Vitamin D*, Elsevier, 2004.
- [2] A.J. Brown, E. Slatopolsky, Vitamin D analogs: therapeutic applications and mechanisms for selectivity, *Mol. Aspect. Med.* 29 (2008) 433–452.
- [3] Y. Wang, J. Zhu, H.F. Deluca, Where is the vitamin D receptor? *Arch. Biochem. Biophys.* 523 (2012) 123–133.
- [4] R. Bouillon, G. Carmeliet, L. Verlinden, E.V. Etten, A. Verstuyf, H.F. Luderer, L. Lieben, C. Mathieu, M. Demay, Vitamin D and human health: lessons from vitamin D receptor null mice, *Endocr. Rev.* 29 (2008) 726–776.
- [5] K.K. Deeb, D.L. Trump, C.S. Johnson, Vitamin D signalling pathways in cancer: potential for anticancer therapeutics, *Nat. Rev. Canc.* 7 (2007) 684–700.
- [6] J.C. Fleet, M. Desmet, R. Johnson, Y. Li, Vitamin D and cancer: a review of molecular mechanisms, *Biochem. J.* 441 (2012) 61–76.
- [7] D. Feldman, A.V. Krishnan, S. Swami, E. Giovannucci, B.J. Feldman, The role of vitamin D in reducing cancer risk and progression, *Nat. Rev. Canc.* 14 (2014) 342–357.
- [8] D. Matthews, E. Laporta, G.M. Zinser, C.J. Narvaez, J. Welsh, Genomic vitamin D signaling in breast cancer: insights from animal models and human cells, *J. Steroid Biochem. Mol. Biol.* 121 (2010) 362.
- [9] M.R. Haussler, G.K. Whitfield, I. Kaneko, C.A. Haussler, D. Hsieh, J.C. Hsieh, P.W. Jurutka, Molecular mechanisms of vitamin D action, *Calcif. Tissue Int.* 92 (2013) 77–98.
- [10] J.W. Pike, M.B. Meyer, K.A. Bishop, Regulation of target gene expression by the vitamin D receptor - an update on mechanisms, *Rev. Endocr. Metab. Disord.* 13 (2012) 45–55.
- [11] K. Dalhoff, J. Dancy, L. Astrup, T. Skovsgaard, K.J. Hamberg, F.J. Lofts, O. Rosmorduc, S. Erlinger, H.J. Bach, W.P. Steward, A phase II study of the vitamin D analogue Seocalcitol in patients with inoperable hepatocellular carcinoma, *Br. J. Canc.* 89 (2003) 252–257.
- [12] S. Srinivas, D. Feldman, J. Reichrath, M. Friedrich, A phase II trial of calcitriol and naproxen in recurrent prostate cancer, *Anticancer Res.* 29 (2009) 3605–3610.
- [13] M.H. Sherman, R.T. Yu, D.D. Engle, N. Ding, A.R. Atkins, H. Tiriach, E.A. Collisson, F. Connor, T.V. Dyke, S. Kozlov, Vitamin D receptor-mediated stromal reprogramming suppresses pancreatitis and enhances pancreatic cancer therapy, *Cell* 159 (2014) 80–93.
- [14] W.K. Hendrickson, R. Flavin, J.L. Kasperzyk, M. Fiorentino, F. Fang, R. Lis, C. Fiore, K.L. Penney, J. Ma, P.W. Kantoff, Vitamin D receptor protein expression in tumor tissue and prostate cancer progression, *Journal of Clinical Oncology Official Journal of the American Society of Clinical Oncology* 29 (2011) 2378.
- [15] M.A. Maestro, F. Molnár, A. Mouriño, C. Carlberg, Vitamin D receptor 2016: novel ligands and structural insights, *Expert Opin. Ther. Pat.* 26 (2016) 1291.
- [16] K.R. Stayrook, M.W. Carson, Y.L. Ma, J.A. Dodge, Chapter 78 - non-secosteroidal ligands and modulators, *Vitamins D* (2011) 1497–1508.
- [17] L.A. Plum, H.F. Deluca, Vitamin D, disease and therapeutic opportunities, *Nat. Rev. Drug Discov.* 9 (2010) 941–955.
- [18] J. Body, D. Niepel, G. Tonini, Hypercalcaemia and hypocalcaemia: finding the balance. *Supportive Care in Cancer Official Journal of the Multinational Association of Supportive Care in Cancer*, 25, 2017, pp. 1639–1649.
- [19] S. Hillel, I.G. Glezerman, Hypercalcemia of malignancy and new treatment options, *Therapeut. Clin. Risk Manag.* 11 (2015) 1779–1788.
- [20] A.E. Mirrakhimov, Hypercalcemia of malignancy: an update on pathogenesis and management, *N. Am. J. Med. Sci.* 7 (2015) 483–493.
- [21] A.F. Stewart, Hypercalcemia associated with cancer — NEJM, *N. Engl. J. Med.* 352 (2005) 373–379.
- [22] Yamada, Sachiko, Makishima, Makoto, Structure–activity relationship of nonsecosteroidal vitamin D receptor modulators, *Trends Pharmacol. Sci.* 35 (2014) 324–337.
- [23] M.F. Boehm, P. Fitzgerald, A. Zou, M.G. Elgort, E.D. Bischoff, L. Mere, D.E. Mais, R.P. Bissonnette, R.A. Heyman, A.M. Nadzan, Novel nonsecosteroidal vitamin D mimics exert VDR-modulating activities with less calcium mobilization than 1,25-dihydroxyvitamin D₃, *Chem. Biol.* 6 (1999) 265–275.
- [24] M. Peräkylä, M. Malinen, K.H. Herzig, C. Carlberg, Gene regulatory potential of nonsteroidal vitamin D receptor ligands, *Mol. Endocrinol.* 19 (2005) 2060.
- [25] W. Shen, J. Xue, Z. Zhao, C. Zhang, Novel nonsecosteroidal VDR agonists with phenyl-pyrrolyl pentane skeleton, *Eur. J. Med. Chem.* 69 (2013) 768–778.
- [26] Z. Ge, M. Hao, M. Xu, Z. Su, Z. Kang, L. Xue, C. Zhang, Novel nonsecosteroidal VDR ligands with phenyl-pyrrolyl pentane skeleton for cancer therapy, *Eur. J. Med. Chem.* 107 (2016) 48–62.
- [27] B. Wang, M. Hao, C. Zhang, Design, synthesis and biological evaluation of nonsecosteroidal vitamin D₃ receptor ligands as anti-tumor agents, *Bioorg. Med. Chem. Lett* 27 (2017) 1428.
- [28] R. Bouillon, W.H. Okamura, A.W. Norman, Structure–function relationship in the vitamin D endocrine system, *Endocr. Rev.* 16 (1995) 200.
- [29] E. Pinard, D. Alberati, E. Borroni, H. Fischer, D. Hainzl, S. Jolidon, J.L. Moreau, R. Narquizian, M. Nettekoven, R.D. Norcross, Discovery of benzoylpiperazines as a novel class of potent and selective GlyT1 inhibitors, *Bioorg. Med. Chem. Lett* 18 (2008) 5134–5139.
- [30] V. Pathak, C.E. Augellizafiran, H.X. Wei, Y. Li, P.G. Oliver, W. Lu, D.J. Buchsbaum, M.J. Suto, Design and synthesis of novel cyclic amine benzimidazoles for the treatment of pancreatic cancer, *J. Med. Chem.* 60 (2017) 7615.
- [31] M. Hao, S. Hou, L. Xue, H. Yuan, L. Zhu, C. Wang, B. Wang, C. Tang, C. Zhang, Further developments of the phenyl-pyrrolyl pentane series of non-steroidal vitamin D receptor modulators as anticancer agents, *J. Med. Chem.* 61 (2018) 3059–3075.
- [32] Z.S. Kang, C. Wang, X.L. Han, J.J. Du, Y.Y. Li, C. Zhang, Design, synthesis and biological evaluation of non-secosteroidal vitamin D receptor ligand bearing double side chain for the treatment of chronic pancreatitis, *Eur. J. Med. Chem.* 146 (2018) 541–553.
- [33] S.J. Shukla, D.T. Nguyen, R. Macarthur, et al., Identification of pregnane X receptor ligands using time-resolved fluorescence resonance energy transfer and quantitative high-throughput screening, *Assay Drug Dev. Technol.* 7 (2009) 143–169.